JOURNAL OF GEOPHYSICAL RESEARCH, VOL. 97, NO. C3, PAGES 3621–3645, MARCH 15, 1992

A Perturbation Simulation of CO_2 Uptake in an Ocean General Circulation Model

JORGE L. SARMIENTO AND JAMES C. ORR

Program in Atmospheric and Oceanic Sciences, Princeton University, Princeton, New Jersey

ULRICH SIEGENTHALER

Physics Institute, University of Bern, Switzerland

The uptake of anthropogenic CO_2 by the ocean is simulated using a perturbation approach in a three-dimensional global general circulation model. Atmospheric pCO_2 is prescribed for the period 1750–1990 using the combined Siple ice core and Mauna Loa records. For the period 1980 to 1989, the average flux of CO_2 into the ocean is 1.9 GtC/yr. However the bomb radiocarbon simulation of Toggweiler et al. (1989*b*) shows that the surface to deep ocean exchange in this model is too sluggish. Hence the CO_2 uptake calculated by the model is probably below the actual value. The observed atmospheric increase in 1980 to 1989 is 3.2 GtC/yr, for a combined atmosphere-ocean total of 5.1 GtC/yr. This is comparable to the estimated fossil CO_2 production of 5.4 GtC/yr, implying that other sources and sinks (such as from deforestation, enhanced growth of land biota, and changes in the ocean carbon cycle) must be approximately in balance. The sensitivity of the uptake to the gas exchange rate is small: a 100% increase in gas exchange rate gives only a 9.2% increase in cumulative oceanic uptake. Details of the penetration into different oceanic regions are discussed.

1. INTRODUCTION

A balanced budget for anthropogenic CO_2 continues to elude the scientific community despite the passing of more than five decades since the papers of *Callendar* [1938, 1940, 1949], who first investigated in a systematic way the increase of CO_2 in the atmosphere. The only relatively firm constraints on this budget are the increase in atmospheric CO_2 measured at monitoring stations since the late 1950's [e.g., *Keeling and Heimann*, 1986; *Keeling et al.*, 1989*a*; *Beardsmore and Pearman*, 1987; *Conway et al.*, 1988] and in ice cores going back two centuries [*Neftel et al.*, 1985; *Friedli et al.*, 1986], and the release of CO_2 by burning of fossil fuels and production of cement [*Rotty and Masters*, 1985; *Marland*, 1989]. By contrast, estimates of the oceanic sink and terrestrial biospheric source due to deforestation and land use change have large uncertainties associated with them. Furthermore, as the Intergovernmental Panel on Climate Change (IPCC) summary of these sources and sinks shows (Table 1) , there remains a large missing sink of 1.6±1.4 GtC/yr [*Houghton et al.*, 1990]. Carbon cycle modelers have generally assumed that the missing sink is terrestrial biota through an enhancement of vegetation growth [e.g., *Siegenthaler and Oeschger*, 1987], but no direct evidence for this exists.

The consensus represented by Table 1 has recently received a severe challenge from the study of *Tans et al.* [1990]. They have produced new estimates of the terrestrial and oceanic sources and sinks by an analysis of atmospheric and oceanic CO_2 observations in combination with a three-dimensional (3-D) model of atmospheric CO_2 transport. Their model of atmospheric CO_2 transport, when constrained by the observed interhemispheric CO_2 gradient, does not permit a large enough interhemispheric transport from the regions of anthropogenic CO_2 production in the northern hemisphere to allow for a significant southern hemisphere ocean sink, a result confirmed by *Keeling et al.* [1989*b*]. The interhemispheric transport is barely adequate to account for the observed southern hemisphere atmospheric CO_2 increase. The northern hemisphere oceanic uptake estimate which Tans et al. obtain from oceanic observations is less than 1 GtC/yr over the period 1981–1987. Thus, they conclude that the total oceanic sink must be less than 1 GtC/yr over the period 1981–1987. This is half the number given in Table 1 and by *Keeling et al.* [1989*b*], and implies that the net imbalance in the carbon budget must necessarily be balanced by a sink of more than 2.6 GtC/yr in the terrestrial biosphere, with much of this uptake occurring in the temperate latitudes of the northern hemisphere.

The estimates of oceanic uptake of CO_2 given in Table 1 come primarily from box models such as the simple one-dimensional box-diffusion and outcrop-diffusion models of *Oeschger et al.* [1975] and *Siegenthaler* [1983], which are calibrated with ocean tracer observations such as natural and bomb radiocarbon. More sophisticated box models also exist, such as those of *Bolin et al.* [1987] (see review by *Baes et al.* [1985]). However, few of these models provide the horizontal spatial resolution at the surface that is needed to better understand the implications of the *Tans et al.* [1990] study. Furthermore, none of these models has realistic physics and they must therefore rely entirely on tracer calibrations for estimating appropriate parameters to represent the effects of ocean circulation, diffusion, and convection. The only published studies that have been carried out with more realistic 3-D ocean general circulation models are those of *Maier-Reimer and Hasselmann* [1987], and *Bacastow and Maier-Reimer* [1990], the latter of which is also discussed in *Volk and Bacastow* [1989], and a calculation presented by *Keeling et al.* [1989*a*]. All these studies make use of the "Hamburg" ocean model originally proposed by *Hasselmann*

Paper number 91JC02849.
0148–0227/92/91JC–02849$05.00

TABLE 1. The 1980–1989 IPCC Budget for CO_2 Perturbation

	Average Perturbation* GtC/yr
Sources	
Fossil	5.4±0.5
Deforestation	1.6±1.0
Total	7.0±1.2
Sinks	
Atmosphere	3.4±0.2
Oceans (Steady State Models)	2.0±0.8
Total	5.4±0.8
Sinks Unaccounted For	1.6±1.4

Taken from *Houghton et al.* [1990].
*1 GtC=10^{12} kg C.

[1982] and developed by *Maier-Reimer et al.* [1982]. They give total CO_2 uptake estimates which are consistent with the simpler models as well as showing a large uptake by the southern hemisphere ocean.

This paper documents the results of a first simulation utilizing a 3-D primitive equation ocean general circulation model based on the approach of *Bryan* [1969] to place further constraints on the role of the ocean in the fossil CO_2 budget. Our long-term strategy involves two parallel approaches. The first assumes that the pre-industrial ocean carbon cycle continues to operate without being affected directly by anthropogenic perturbations. This "steady state" approach, which all modelers have taken up to now, enables us to assume that anthropogenic CO_2 can essentially be treated as a passive tracer not involved in biological processes. It excludes the possibility that the oceanic carbon cycle may respond dynamically to the effect of the anthropogenic greenhouse gas perturbations on climate. However, previous box-modeling studies have shown that changes in the oceanic carbon cycle are capable of causing quite large perturbations in atmospheric CO_2 [e.g., *Knox and McElroy*, 1984; *Sarmiento* and *Toggweiler*, 1984; *Siegenthaler and Wenk*, 1984; *Sarmiento et al.*, 1988; *Peng and Broecker*, 1991; *Joos et al.*, 1991]. Consideration of these effects (our second approach) is left to future work.

The steady state approach of calculating atmospheric CO_2 uptake by the oceans requires three essential ingredients. First is an ocean circulation model. Here we have used a primitive equation 3-D ocean general circulation model with annual mean forcing. Second, a model for the carbonate chemistry in surface water is required so that the partial pressure of CO_2 (pCO_2) can be related to the total CO_2 concentration (ΣCO_2) in seawater. We take a perturbation approach, assuming that the mechanisms and rates of the processes affecting the natural cycling of carbon in the ocean are not affected by the anthropogenic CO_2 increase. This enables us to consider only the perturbation of ΣCO_2, the species of interest in the present context. Finally, one needs a time history for the atmospheric CO_2 perturbation to serve as a boundary condition. In earlier studies, anthropogenic emissions into the atmosphere were usually prescribed, and the increase in atmospheric and oceanic CO_2 were obtained from a model. *Siegenthaler and Oeschger* [1987]; and *Keeling et al.* [1989*a*], on the other hand, prescribe the atmospheric CO_2 history using measurements of CO_2 from ice core analyses and direct atmospheric observations, and use a model to estimate the oceanic uptake. We follow the latter approach.

The role of the terrestrial biota is not explicitly considered here. However, an estimate of the total net emission into the atmosphere from fossil, biota, and other sources and sinks can be obtained by summing the rate of CO_2 accumulation observed in the atmosphere to that predicted by the ocean model. By subtracting the fossil CO_2 production numbers, an estimate of the net contribution from the biota plus other sources minus sinks can be obtained. The reliability of this estimate depends on the reliability of the ocean model (including the assumption of an unchanging natural carbon cycle), the reliability of fossil CO_2 production rate estimates, and the representativity of the ice core results for the atmospheric CO_2 history.

Our simulation gives an average oceanic fossil CO_2 uptake of 1.9 GtC/yr for the period 1980–1989, in agreement with previous work summarized in Table 1. We present arguments below that lead us to believe that this uptake estimate is most likely a lower limit. We discuss the implications of this result for the *Tans et al.* [1990] study. As a first step towards examining the sensitivity of this result to various factors such as the gas exchange rate, ocean circulation and chemistry, we report here on a series of simulations that reveal little sensitivity of oceanic CO_2 uptake to gas exchange rate.

2. Model Description

Ice core measurements show that the atmospheric CO_2 concentration varied by no more than 10 ppm for ~1000 years prior to 1800 [*Siegenthaler et al.*, 1988; also see *Raynaud and Barnola*, 1985], implying that the carbon cycle was approximately in steady state. This evidence for a pre-industrial steady state supports the perturbation approach for simulating oceanic uptake of anthropogenic CO_2 , which assumes that the natural cycling of carbon in the oceans has continued unchanged despite the anthropogenic increase, and in particular, that the biological fluxes have remained constant. In the oceans, a steady state requires that the concentration of dissolved inorganic carbon, ΣCO_2, be constant when averaged over several years, thereby smoothing out seasonal variability and interannual variability such as that caused by El Niño. The pre-industrial steady state can be represented by $\partial \Sigma CO_{2,0}/\partial t = 0$, where $\Sigma CO_{2,0}$ is the annually averaged pre-industrial total carbon concentration at a given location in the ocean. Assuming that $\partial \Sigma CO_{2,0}/\partial t$ continues to be 0 today, the conservation equation for perturbation ΣCO_2 which we solve can be written as

$$\frac{\partial(\Sigma CO_2 - \Sigma CO_{2,0})}{\partial t} = \frac{\partial \delta \Sigma CO_2}{\partial t} = -\vec{V} \cdot \vec{\nabla} \delta \Sigma CO_2 + \vec{\nabla} \cdot (D \vec{\nabla} \delta \Sigma CO_2) + \delta SMS \quad (1)$$

with $\delta \Sigma CO_2$ defined as $\Sigma CO_2 - \Sigma CO_{2,0}$ (see Table 2). The term δSMS is the deviation of the nontransport (i.e., chemical and biological) sources minus sinks from their natural values; it affects just the perturbation total carbon distribution. Since we assume that the biogenic particle fluxes have not changed, $\delta SMS = 0$ in all layers but the surface, where

TABLE 2. Definitions

Parameter	Value
$\delta\Sigma CO_2$	$\Sigma CO_2 - \Sigma CO_{2,0}$*
δpCO_2	$pCO_2 - pCO_{2,0}$†
ΔpCO_2	$pCO_{2_{oc}} - pCO_{2_{atm}}$
$\Delta\delta pCO_2$	$\Delta pCO_2 - \Delta pCO_{2,0}$‡
	$\delta pCO_{2_{oc}} - \delta pCO_{2_{atm}}$

*The δ is used to indicate the cumulative change at time t relative to pre-anthropogenic or to the beginning of a simulation at time 0, both symbolized by the subscript 0.

†This definition for δpCO_2 differs from that of *Maier-Reimer and Hasselmann* [1987], who use δpCO_2 as a symbol for our $\Delta\delta pCO_2$.

‡The $\Delta\delta pCO_2$ is that portion of the air-sea difference at time t that is directly attributable to the atmospheric perturbation. This is the same notation used by *Volk and Bacastow* [1989].

$\delta SMS = f_{\delta CO_2}/\Delta z_1$. $f_{\delta CO_2}$ is the net flux of excess CO_2 from the atmosphere to the ocean. The value Δz_1=51 m is the thickness of the model's top layer (see Table 3).

We use advection ($\vec{V}$), diffusion (D), and convection fields based on the nonseasonal prognostic world ocean model developed by *Toggweiler et al.* [1989*a*, model P]. Convection in the model is the homogenization of adjacent layers that are unstable with respect to each other. *Toggweiler et al.* [1989*a*] obtain their flow field from a solution of the equations of motion as modified by the Boussinesq and hydrostatic approximations, and the equations of continuity, conservation of salinity and potential temperature, and state. The numerical method of *Bryan* [1969] is used, modified to include longer time steps with increasing depth as described by *Bryan* [1984] to accelerate convergence to a solution. A longer time step is also obtained by zonally filtering the horizontal tracer field poleward of 46.732° latitude, and the velocity field poleward of 80.1°, as described by *Bryan et al.* [1975]. The model has a north-south resolution of 4.5°, an east-west resolution of 3.75°, and a maximum depth of 5000 m resolved by 12 levels in the vertical as shown in Table 3. The bathymetry is as realistic as permitted by the resolution.

TABLE 3. Model Layer Depths

Model Layer	Depth of Layer, m	
	Midpoint	Bottom
1	26	51
2	85	119
3	170	220
4	295	371
5	483	595
6	755	914
7	1131	1347
8	1622	1898
9	2228	2559
10	2935	3311
11	3721	4131
12	4565	5000

The annual mean wind stress of *Hellerman and Rosenstein* [1983] provides the upper boundary condition used by *Toggweiler et al.* [1989*a*] to solve the equations of motion, with the vertical velocity, w, set to zero at the air-sea interface to filter out gravity waves. A linear drag on the horizontal velocity is specified at the bottom, with a no-slip condition applied at lateral boundaries. Temperature and salinity have no flux permitted across any of the boundaries, but in the surface layer the temperature and salinity fields are forced towards the annual mean observed fields of *Levitus* [1982] with a time scale of 30 days. Sub-grid scale motions are represented by an eddy viscosity for momentum of 20 cm^2s^{-1}in the vertical and 2.5x10^9 cm^2s^{-1}in the horizontal, a vertical eddy diffusivity (for tracers) which varies smoothly between 0.3 cm^2s^{-1}in the upper kilometer and 1.3 cm^2s^{-1} in the deepest layer, and a horizontal eddy diffusivity which decreases from 1.0 to 0.5x10^7 cm^2 s^{-1} from surface to bottom. The ocean circulation model was run for 2009 years by *Toggweiler et al.* [1989*a*] using a time step of 1/300 year. Further details of the model are given in *Toggweiler et al.* [1989*a*] and in section 3.

Najjar [1990] ran *Toggweiler et al.'s* [1989*a*] model P for an additional 55 years to produce time-averaged velocity fields obtained by averaging 17 samplings during the 55-year run. Convection in the *Toggweiler et al.* [1989*a*] model is implemented by homogenizing adjacent layers if they are unstable with respect to each other. A convection index was obtained by averaging over the entire 55-year run. With 300 time steps per year, and two passes through the convection routine per time step, the total 55-year sample represents 33,000 passes through the convection routine. The convection index is the fraction of those 33,000 passes during which convection actually occurs at a given grid point.

Our perturbation simulations make use of *Najjar*'s [1990] average velocity field and convection indices in an "off-line" version of the model that requires substantially fewer computer resources due to the fact that only the tracer conservation equation is solved. Convection is most easily dealt with by specifying that it never occur, that it occur one pass per time step, or that it occur two passes per time step. We follow *Najjar*'s [1990] lead by specifying no convection in our perturbation carbon simulation if the convection index is 0 to 1/3, one pass through the convection routine per time step if the convection index is 1/3 to 2/3, and two passes per time step if the index is 2/3 to 1. Resolution and topography of the model are identical to *Toggweiler et al.'s* [1989*a*], as is the subgrid-scale vertical and horizontal eddy diffusivity. We use the same numerical method as Toggweiler et al., including filtering of the tracer equations poleward of 46.732° as described by *Bryan et al*. [1975], but not including accelerated time stepping in the deep ocean for CO_2, since this approach is not appropriate for a time-dependent problem. As might be expected, the off-line model does not exactly reproduce the behavior of the fully predictive "on-line" model, which solves the equations of motion, continuity, conservation of salinity and potential temperature as well as state. The off-line model takes up 10.4% more bomb radiocarbon than the on-line model in a comparison study carried out by B. Samuels (personal communication,

1991). Most of the enhanced uptake in the off-line model occurs in high latitude regions of deep convection, suggesting that the off-line convective parameterization is at fault.

The on-line version of the model has been used by *Toggweiler et al.* [1989*a*, *b*] for simulating the oceanic distribution of radiocarbon. They found generally good agreement between simulated and observed distributions. However, the uptake of bomb-produced radiocarbon predicted by the model was 16% lower than the observations, indicating that the ventilation of the thermocline is too sluggish. This underprediction of bomb radiocarbon uptake is partially offset in the off-line version which, as previously noted, takes up 10.4% more bomb radiocarbon than the on-line version. It is difficult in a 3-D ocean circulation model to adjust the vertical exchange, so we use the model being aware of these problems.

The perturbation flux, $f_{\delta CO_2}$, from atmosphere (atm) to ocean (oc) is given by

$$\begin{aligned} f_{\delta CO_2} &= k_w \alpha (1-\gamma_{ice})(\delta pCO_{2atm} - \delta pCO_{2oc}) \\ &= k_g (1-\gamma_{ice})(\delta pCO_{2atm} - \delta pCO_{2oc}) \\ &= -k_g (1-\gamma_{ice}) \Delta \delta pCO_2 \end{aligned} \quad (2)$$

with $f_{\delta CO_2}$ in mol $m^{-2}yr^{-1}$, where k_w is the transfer velocity in m yr^{-1}, α is the solubility of CO_2 in mol m^{-3} ppm^{-1}, k_g is the gas-phase related transfer coefficient in mol $m^{-2}yr^{-1}ppm^{-1}$, δpCO_2 is $pCO_2 - pCO_{2,0}$, with the subscript 0 indicating pre-industrial (see Table 2); and pCO_2 is the partial pressure of CO_2 in ppm. The fraction of sea ice cover γ_{ice} is obtained from *Alexander and Mobley* [1976]. In the model the flux through a given grid point is calculated by taking the product of $\Delta\delta pCO_2$ for that grid point with the average k_g over the entire area covered by the grid point, then correcting the product for the fraction of the area which is covered by ice. In (2), the different conditions determining the gas flux are separated: k_g summarizes the physical factors, in particular, wind speed and temperature, while the terms within the last set of parentheses describe the concentration difference across the air-sea interface, i.e., the chemical driving force. In order to solve (2) we need to specify k_g , δpCO_{2atm}, and δpCO_{2oc}, each of which is discussed in turn.

2.1. *Gas Transfer Coefficient*

We use the same gas exchange rate as the natural radiocarbon simulation of *Toggweiler et al.* [1989*a*]. However, Toggweiler et al.'s expression for gas exchange, obtained from *Broecker et al.* [1985*a*], was revised to take into consideration the fact that atmospheric pCO_2 increases during the course of our simulation. Broecker et al. give, for the CO_2 flux, the expression

$$f_{CO_2} = \kappa \left(1 - \frac{pCO_{2oc}}{pCO_{2atm}}\right) \quad (3)$$

with

$$\kappa = \kappa_0 (U-2) \quad (4)$$

where U is wind speed in m s^{-1} and κ_0 is a constant. A comparison of (2) with (3) shows that (3) has pCO_{2atm} included in κ. This does not present a problem so long as the atmospheric pCO_2 is constant, but such is not the case in our simulations. We thus take the form of (2) in combination with (3) to obtain an appropriate expression for k_g in terms of κ and pCO_{2atm}:

$$k_g = \frac{\kappa}{pCO_{2atm}} = \frac{\kappa_0}{pCO_{2atm}}(U-2) \quad (5)$$

Toggweiler et al. [1989*a*, *b*] used a value for κ_0 of 3.5 mol m^{-2} yr^{-1}. To determine k_g, we need the pCO_2 value corresponding to this κ_0. In order to remain consistent with the prebomb radiocarbon study of *Toggweiler et al.* [1989*a*] this study sets pCO_{2atm}= 280 ppm in dry air as the pre-industrial reference value. After correcting for moist air above the ocean, this partial pressure reduces to between approximately 269 and 278 ppm for water temperatures of 30 °C to 0 °C, respectively (see below). Since most of the radiocarbon enters the oceans in colder waters [*Toggweiler et al.*, 1989*a*], a value of ~275 ppm seems appropriate. Thus the gas exchange coefficient in our model is

$$k_g = \frac{\kappa}{275 \text{ ppm}} = k_{g0}(U-2) \quad (6)$$

with k_{g0}= 3.5 mol m^{-2} yr^{-1}/275 ppm = 0.0127 mol m^{-2} yr^{-1} ppm^{-1}. Annual mean wind speeds for evaluating (6) are taken from *Esbensen and Kushnir* [1981]. They give data only over ice-free ocean. These data were used to estimate wind speeds over ice-covered regions by means of a Laplacian filling algorithm. The global average value of k_g obtained in this way is 0.065 mol m^{-2} yr^{-1} ppm^{-1}, corresponding to 17.9 mol m^{-2} $yr^{-1}$with the pCO_2 at the pre-industrial moisture corrected value of 275 ppm as used above.

The bomb radiocarbon study of *Toggweiler et al.* [1989*b*] used exactly the same κ_0 as for the prebomb simulation, i.e., 3.5 mol m^{-2} yr^{-1}. Bomb radiocarbon began entering the ocean when the pCO_2 was already in the range 310 to 320 ppm; hence internal consistency would have required that *Toggweiler et al.* [1989*b*] use a κ_0 of approximately (3.5 mol $m^{-2}yr^{-1}$)(315 ppm/280 ppm) = 3.94 mol $m^{-2}yr^{-1}$. The dependence on pCO_2 is included explicitly in our model; thus the comparison of our study with the bomb radiocarbon simulation of *Toggweiler et al.* [1989*b*] must take into account that the gas exchange rate in the latter study is smaller by ~11%.

Dependence of the gas transfer coefficient ($k_g = k_w\alpha$) on temperature is neglected. Although both the transfer velocity (k_w) and solubility (α) are highly temperature dependent according to *Liss and Merlivat*, [1986] and *Weiss*, [1974], respectively, their effects are opposite and tend to cancel. The temperature sensitivity of k_g is of the order of ±10% around the gas exchange rate at 20°C [*Siegenthaler*, 1986; *Etcheto and Merlivat*, 1988].

2.2. *Boundary Condition for Atmospheric CO_2*

The pCO_{2atm} is prescribed from 1750 to 1990 using an update of *Siegenthaler and Oeschger's* [1987] spline fit to the Siple ice core data of *Neftel et al.* [1985] and *Friedli et al.* [1986] combined with the Mauna Loa record of *Keeling et al.* [1989*a*] (see Figure 1*a*). The spline fit uses observations to 1988 and is extrapolated to 1990. The pCO_2 at the beginning of the simulation, $pCO_{2,0}$, is taken as 280 ppm such that

$$\delta pCO_{2atm} = pCO_{2atm} - 280 \text{ ppm} \quad (7)$$

The atmospheric CO_2 concentration is given by convention as the partial pressure in dry air. For calculating the

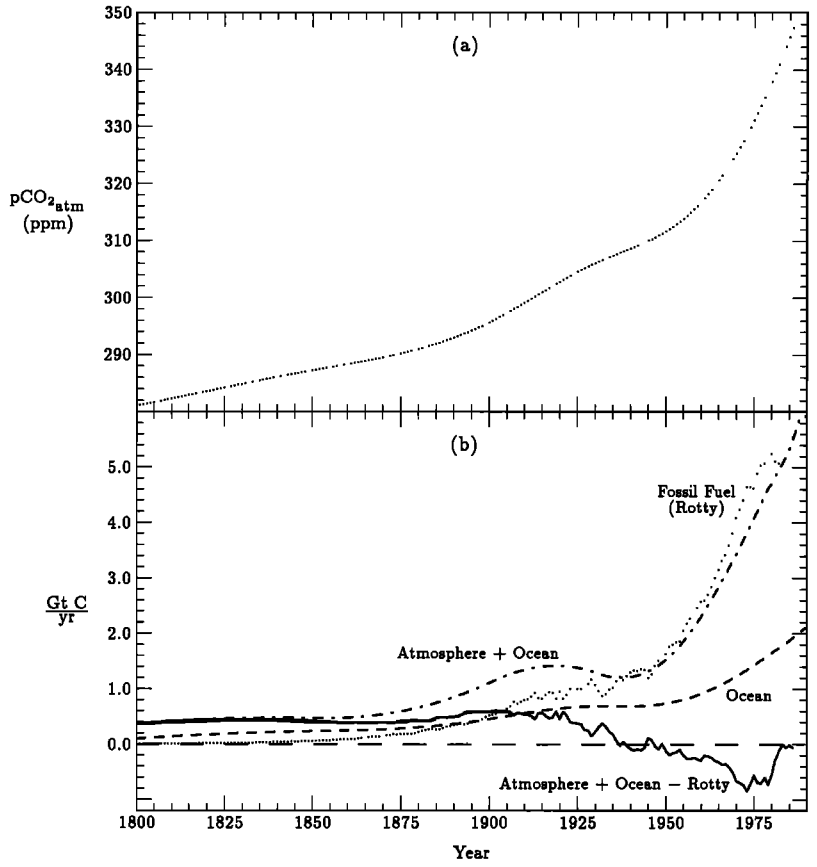

Fig. 1. (*a*) Spline fit to the Siple ice core/Mauna Loa atmospheric pCO_2 which is used to force the simulation. (*b*) The annual change in carbon calculated by version A1.1 of the 3-D ocean model, summed to the annual change in the atmospheric inventory. The atmospheric inventory is based on the Siple ice core and Mauna Loa CO_2 data as analyzed by *Siegenthaler and Oeschger* [1987]. The fossil CO_2 production is taken from *Rotty and Masters* [1985] with updates by *Marland* [1989]. The difference between the combined atmosphere/ocean change and the "Fossil" curve shows what the net release from sources other than those modeled would have to be if the ocean model were correct. Note, in particular, that the present model requires an additional source of carbon prior to ~1940, and a sink after that.

air-sea gas exchange, it must be corrected to the appropriate pressure in moist air at 100% water vapor saturation at the temperature of the surface water. We use the expression given by *Siegenthaler* [1986]:

$$pCO_2 = pCO_{2,\mathrm{dry}}(1 - e_s/p_a) \tag{8}$$

where e_s is the saturation water vapor pressure and p_a the barometric pressure at sea level. For sea water, we obtain the following approximation, using p_a= 1013 mbar and noting that e_s(sea water) = 0.981 e_s(pure water):

$$\ln(e_s/p_a) = 20.1050 - 0.0097982 \cdot T_{abs} - 6163.10/T_{abs} \tag{9}$$

where T_{abs} is absolute temperature. The surface ocean temperature used for this calculation is the average value of *Toggweiler et al.* [1989*a*] as obtained by *Najjar* [1990] in the same way the velocity field averages were obtained. This is close to the annual mean of *Levitus* [1982], which is the temperature used in forcing the ocean circulation model. The overall correction to the pCO_2 due to the moist air correction is between ~0.5 and 4.0%, depending on the saturation water vapor pressure, and therefore on temperature.

2.3. *Determination of* $\delta pCO_{2_{OC}}$

Solution of (1) gives $\delta\Sigma CO_2 = \Sigma CO_2 - \Sigma CO_{2,0}$, from which we must calculate $\delta pCO_{2_{OC}} = pCO_{2_{OC}} - pCO_{2,0_{OC}}$ (see Table 2 for definitions). When the ratio $\delta pCO_{2_{OC}}/\delta\Sigma CO_2$, as calculated from the carbonate equilibria, is plotted versus $\delta pCO_{2_{OC}}$ for a given temperature (and constant alkalinity), a remarkably linear relation is found over a range in excess of $\delta pCO_{2_{OC}}$= 0 to 200 ppm. This means that instead of explicitly solving the relatively complex carbonate equilibria each time step at each surface grid point, we can approximate the relation between $\delta pCO_{2_{OC}}$ and $\delta\Sigma CO_2$ very well by an analytical expression. This approach is equivalent to the buffer factor approach used in 1-D models, but somewhat simpler for 3-D calculations, since the buffer factor approach would require $\Sigma CO_{2,0}$ to be specified over the whole ocean. Given this, we can write

$$\frac{\delta pCO_{2_{OC}}}{\delta\Sigma CO_2} = \frac{pCO_{2_{OC}} - pCO_{2,0_{OC}}}{\Sigma CO_2 - \Sigma CO_{2,0}} = z_0 + z_1 \delta pCO_{2_{OC}} \tag{10}$$

where

$$z_0 = 1.7561 - 0.31618 \cdot T + .0004444 \cdot T^2$$

and

$$z_1 = 0.004096 - 7.7086 \times 10^{-5} \cdot T + 6.10 \times 10^{-7} \cdot T^2$$

are obtained as explained below. The parameter $\delta pCO_{2_{OC}}$ is in ppm, $\delta\Sigma CO_2$ is in μmol kg^{-1}, and T is in °C. Rearranging (10) gives

$$\delta pCO_{2_{OC}} = \frac{z_0 \delta\Sigma CO_2}{1 - z_1 \delta\Sigma CO_2} \tag{11}$$

The coefficients z_0 and z_1 are obtained as follows. The $pCO_{2,0_{OC}}$ can be specified with adequate accuracy from equilibrium thermodynamic relationships by knowing ΣCO_2, alkalinity, temperature, and salinity. Temperature is given by the model simulation. We approximate the preindustrial surface ocean by imposing a uniform salinity of 35 $^{\circ}/_{\circ\circ}$ and an alkalinity of 2300 μeq kg^{-1}, and taking the ocean $pCO_{2,0}$ to be in equilibrium with an atmospheric CO_2 concentration of 280 ppm everywhere. Using these quantities, a corresponding $\Sigma CO_{2,0}$ is calculated using the subroutine of *Bacastow* [1981], the *Lyman* [1956] equilibrium constants [*Takahashi et al.*, 1976] and the CO_2 solubilities of *Weiss* [1974]. This yields $\Sigma CO_{2,0}$ as a function of temperature. The ΣCO_2 is then increased incrementally and the pCO_2 is calculated. The final table relating the ΣCO_2 and pCO_2 to each other and to temperature is then used in conjunction with $pCO_{2,0}$ and $\Sigma CO_{2,0}$ estimated as explained above to obtain z_0 and z_1.

The final equation (11) fits the exactly calculated values of $\delta pCO_{2_{OC}}$ to better than 1% at $\delta pCO_{2_{OC}} \leq 200$ ppm. This approximation was compared by *Fink* [1991] to the full equilibrium equations given in *Peng et al.* [1987], using the carbonic acid dissociation constants of *Mehrbach et al.* [1973] and *Goyet and Poisson* [1989]. The difference is largest at low temperatures. At 0°C, (11) deviates by 3 to 4% from the Mehrbach et al. calculations, and by −2 to −3% from the Goyet and Poisson calculations. At $T \geq 10$°C, the differences are smaller than $\pm$ 1%. Since areas with $T \approx 0$°C cover a small fraction of the world ocean, the overall effect of the uncertainties in the chemical equilibrium constants on the calculated ocean uptake is minor. A more detailed consideration of ocean chemistry is left for the future.

Our perturbation approach neglects the fact that surface alkalinity is not quite constant, and $pCO_{2_{OC}}$ is not everywhere in equilibrium with the atmosphere. We consider the influence of this approximation to be small. Inclusion of these effects requires a model with biology, a step planned for the future.

The final expression for the gas flux is obtained by substituting (7) and (11) into (2) and including the moist air correction (8),

$$f_{\delta CO_2} = k_g(1-\gamma_{ice})\left[(pCO_{2_{atm}} - 280 \text{ ppm})(1-e_s/p_a) - \frac{z_0 \delta\Sigma CO_2}{(1 - z_1 \delta\Sigma CO_2)}\right] \quad (12)$$

where k_g is given by (6), γ_{ice} is given by *Alexander and Mobley* [1976], $pCO_{2_{atm}}$ is given by our update of *Siegenthaler and Oeschger's* [1987] Siple ice core/Mauna Loa analysis (Figure 1*a*), e_s/p_a is given by (9), $\delta\Sigma CO_2$ is calculated by the 3-D model using equation (1) with an initial condition of zero everywhere, and z_0 and z_1 are given by (10).

3. Results and Discussion

Table 4 summarizes simulations performed with the model. Simulation A1.1 is denoted as the standard model and is described in detail in section 2. Prior to the ice core atmospheric pCO_2 measurements of *Neftel et al.* [1985] and *Friedli et al.* [1986], it was not possible to prescribe the atmospheric pCO_2 levels before 1958 with any confidence. Simulations of the anthropogenic CO_2 increase were thus generally made with combined models of the ocean and atmosphere, with the input to the atmosphere prescribed using estimates of anthropogenic CO_2 release. For purposes of comparison with earlier studies, we have done one simulation, A1.2, which uses the fossil CO_2 production rates as estimated for the period 1860 to 1986 by *Rotty and Masters* [1985] and *Marland* [1989]. These production rates are extrapolated back in time exponentially to 1800 using a log-linear fit of the data between 1860 and 1986. Other simulations were done with the standard boundary condition to study the sensitivity of the CO_2 uptake to the gas exchange rate and will be discussed in section 3.5.

TABLE 4. List of Simulations

	Description
A1.1	"Standard" simulation using prescribed atmospheric pCO_2
A1.2	Simulation with prescribed fossil CO_2 production rate
	Gas Exchange Sensitivity Studies
A2.1	k_g =1.2 x standard
A3.1	k_g =2.0 x standard
A4.1	Spatially constant k_g equal to standard average
A5.1	k_g from *Liss and Merlivat* [1986]
A6.1	k_g from *Maier-Reimer and Hasselmann* [1987]

A radiocarbon model validation study of the on-line version of our 3-D ocean circulation model has been carried out by *Toggweiler et al.* [1989*a*, *b*]. Results from this work are discussed in connection with our attempts to understand the differences between our model results and simulations carried out by others using the "Hamburg" model (section 3.2). In section 3.5, we further discuss studies of the sensitivity of radiocarbon uptake to gas exchange which were carried out by *Toggweiler et al.* [1989*b*]. These studies show that an increased gas exchange coefficient gives an increased total uptake of bomb radiocarbon which is in better agreement with observations. However, the surface radiocarbon concentrations obtained with this simulation are too high, suggesting that the vertical exchange in the model is too sluggish. We argue that this implies that our estimates of oceanic uptake of anthropogenic CO_2 are most likely a lower limit.

3.1. *Global Oceanic CO_2 Uptake and Regional Distributions*

Figure 1*b* summarizes the cumulative oceanic and atmospheric inventories for our "standard" A1.1 simulation with prescribed atmospheric CO_2 concentrations. *Siegenthaler and Oeschger* [1987] and *Keeling et al.* [1989*a*] discuss similar figures which they obtained from their studies. Already in the early nineteenth century, a relatively large annual input to the atmosphere is necessary in order to explain the atmospheric CO_2 concentration increase at that time (cf. Figure 1*a*). It is very likely that there were major CO_2 emissions from deforestation starting before 1800, a point which has been discussed in detail by *Siegenthaler and Oeschger* [1987]. Note that the validity of this conclusion depends critically on the assumption that the Siple ice core record used in obtaining Figure 1*a* truly reflects the pre-Mauna Loa CO_2 history.

More recently, i.e., nearly every year after 1941, the combined oceanic and atmospheric uptake of carbon by model

A1.1 is less than the fossil production as estimated by *Rotty and Masters* [1985] and *Marland* [1989] (see Figure 1*b*). From mid-1958 to mid-1986, a period of time for which the atmospheric CO_2 record and fossil CO_2 production are strongly constrained, the combined atmospheric and oceanic increase of 104.4 GtC (1 Gt = 10^{12} kg) is 9.6% lower than the estimated fossil CO_2 production of 115.6 GtC. The ocean model would need to take up 29.5% more CO_2 in order to account for just the fossil source between 1958 and 1986. On top of this, we must account for a deforestation source. Our model thus agrees with most previous work in suggesting that the oceanic uptake plus the atmospheric increase cannot account for all the carbon released to the atmosphere by fossil production, deforestation, and land use changes.

From the mid-1970s onwards, the residual flux obtained by subtracting the fossil production from the total atmosphere + ocean accumulation rate, increases from a sink of approximately −0.8 to 0 GtC/yr. *Keeling et al.'s* [1989*a*] analysis of this portion of the curve suggests that perhaps half of this surge may be explained by oceanic warming that occurred during that time. The remainder of the surge is most likely due to an increase in biospheric destruction by human activities, or by local climate changes not accounted for in using the global average temperature.

We turn now to a more detailed consideration of the results. Figure 2*a* shows that there is a very large variation in the zonally averaged perturbation CO_2 flux per unit area of ice-free ocean. From (2) we see that the flux is the product of the gas transfer coefficient, k_g , and air-sea $\Delta\delta pCO_2$ difference. The zonal average of both these quantities over the ice free ocean is shown in Figure 2*a*, from which we can readily infer that the flux is most strongly correlated with

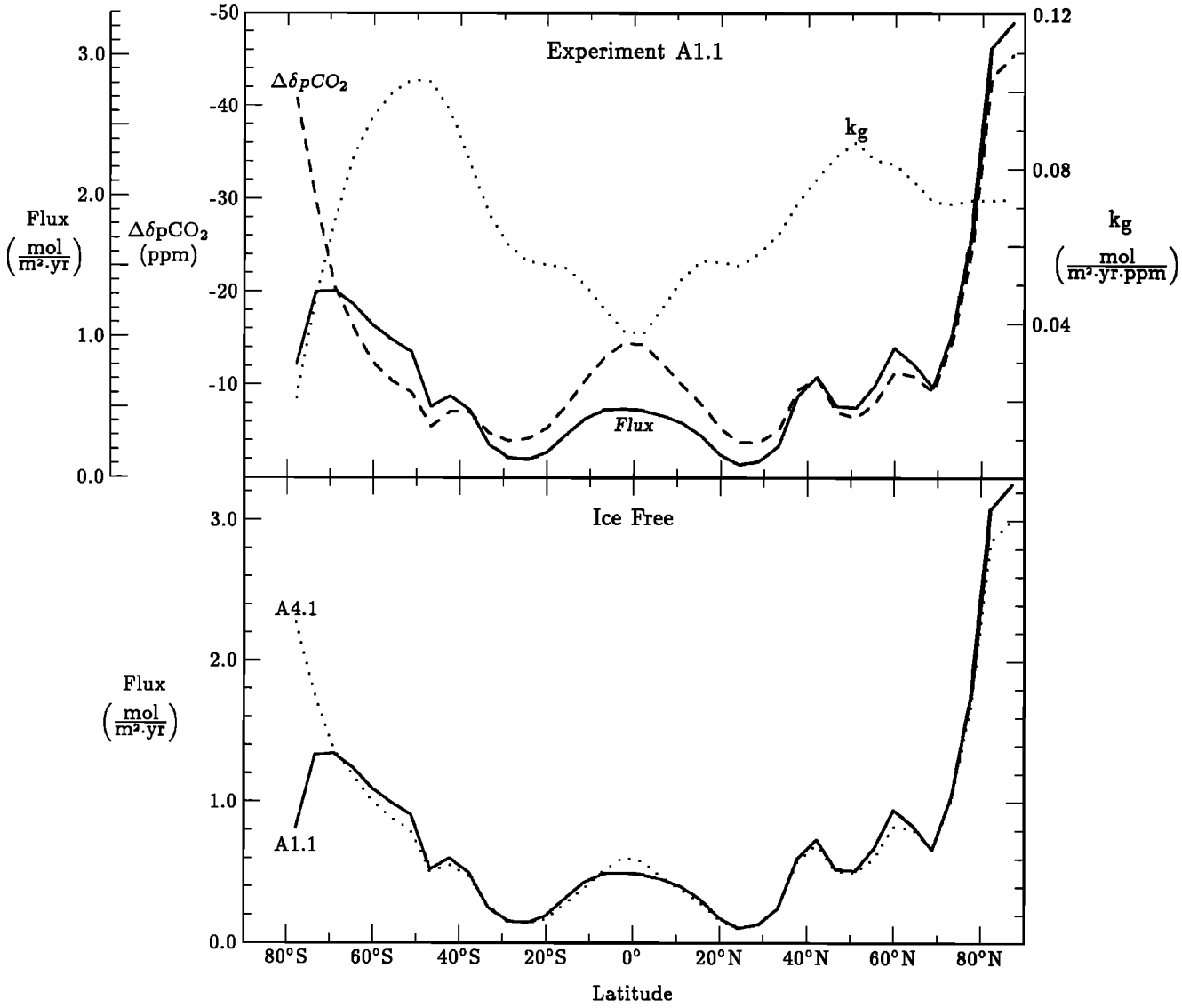

Fig. 2. (*a*) The zonal mean annual flux in 1986 in mol per m^2 of ice free ocean for version A1.1. Also included in the figure are the zonal mean gas transfer coefficient in mol m^{-2} yr^{-1} ppm^{-1}(also per unit area of ice free ocean), and $\Delta\delta pCO_2$ for 1986 in ppm, which together determine the perturbation flux. The large values of $\Delta\delta pCO_2$ in the high latitudes are a result of the ice cover, which prevents the ocean and atmosphere from equilibrating with each other. The flux follows $\Delta\delta pCO_2$ closely, except where k_g becomes very small, near the Antarctic, and, to a lesser extent, at the Equator. (*b*) Version A1.1 zonal mean annual flux per unit area of ice free ocean compared with A4.1, which has a uniform gas exchange coefficient equal to the average of A1.1's coefficient.

$\Delta\delta pCO_2$, except south of ~70°S, where the gas transfer coefficient falls off rapidly with decreasing wind speed. The fall off in wind speed to the south of 70°S occurs primarily in ice-covered regions for which *Esbensen and Kushnir* [1981] give no data. The Laplacian algorithm which was used to fill in these regions extrapolates the decreasing wind speed trend which exists in ice-free regions, giving values which are most likely too low. The effect of these low wind speeds on the total CO_2 uptake is negligible, since most of this area is covered by ice, so that the total flux there is small (cf. Figure 6). The dominance of $\Delta\delta pCO_2$ in determining the pattern of the CO_2 flux is borne out by the results of simulation A4.1, shown in Figure 2*b*. Simulation A4.1 has a uniform k_g equal to the average k_g in the standard A1.1 simulation. The difference between A4.1 and A1.1 is very small except south of ~70°S.

The pattern of $\Delta\delta pCO_2$ derives primarily from the different rates at which convective overturning and upwelling supply the surface with water relatively uncontaminated in perturbation CO_2. Maps of upwelling and convective overturning from this model (Figure 3) exhibit the familiar features of equatorial and subpolar upwelling as well as high-latitude convection. These regions all show high values of the air-sea difference $\Delta\delta pCO_2$ (Figures 2*a* and 4*a*). An additional factor influencing $\Delta\delta pCO_2$ is ice cover. The regions of extremely high air-sea differences in the high latitudes have ice cover that impedes exchange with the atmosphere. In the model this is dealt with by reducing the gas exchange coefficient by a fractional amount equal to the fractional amount of annual mean ice cover. The effect of this reduced gas exchange in maintaining high air-sea $\Delta\delta pCO_2$ differences is compounded further by lateral exchange between ice-covered and ice free water, which provides the ice free regions with a large supply of uncontaminated water.

The flux pattern also depends on the gas transfer coefficient pattern, which, in turn, depends on the wind speed. The high fluxes obtained in high-latitude temperate and subpolar regions are partly a consequence of the high gas exchange coefficients resulting from the high winds in these regions (Figure 2*a*). The $\Delta\delta pCO_2$ pattern, which mainly reflects vertical oceanic exchange, shifts the high flux region towards high latitudes relative to the meridional distribution of the gas exchange coefficient. The most marked influence of the gas transfer coefficient is found in the low wind speed region south of 70°S.

It is important to recognize that although the absolute air-sea difference in pCO_2, ΔpCO_2 (a quantity which can be directly measured), does determine net air-sea exchange of CO_2, it cannot be used as a direct indicator of where the anthropogenic CO_2 is entering the ocean. For that, we require the difference between the air-sea pCO_2 perturbation, at present and prior to the beginning of significant anthro-

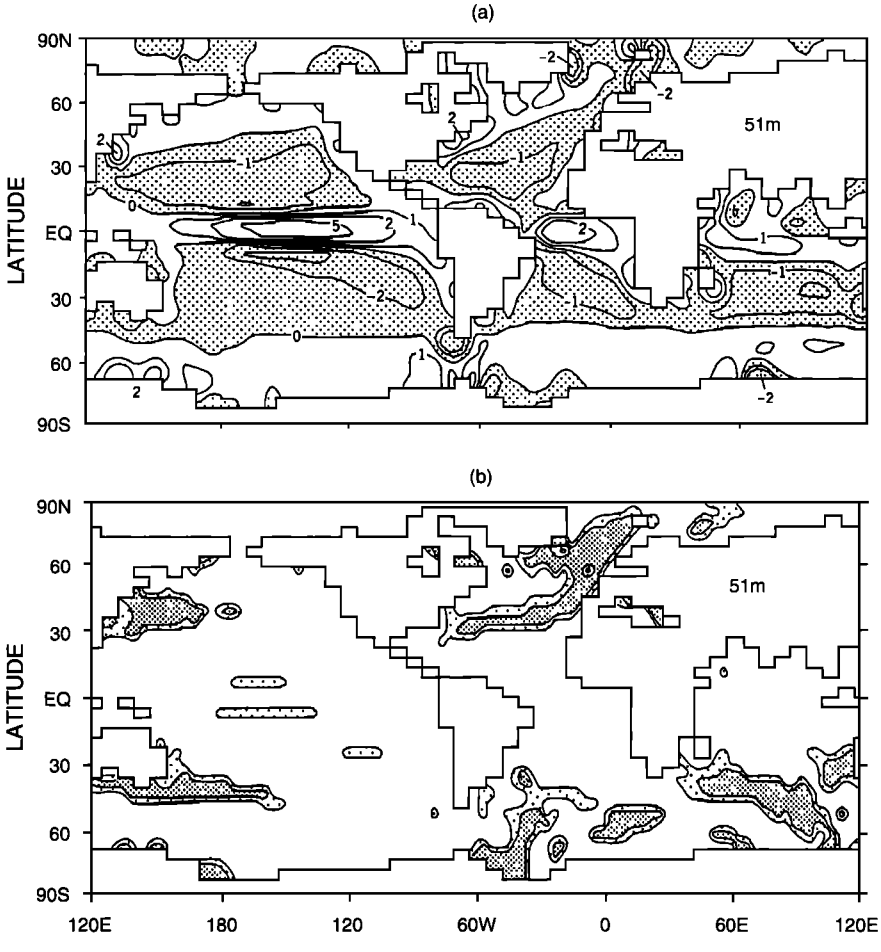

Fig. 3. Maps from *Toggweiler et al.* [1989*a*] showing (*a*) vertical velocity and (*b*) the convective index at 51 m in their ocean circulation model P. Upwelling is given in units of 10^{-6} m s^{-1}, with downwelling areas indicated by stippling. Light and dense stippling in Figure 3*b* indicate convective overturning greater than 25% and 75% of the time, respectively.

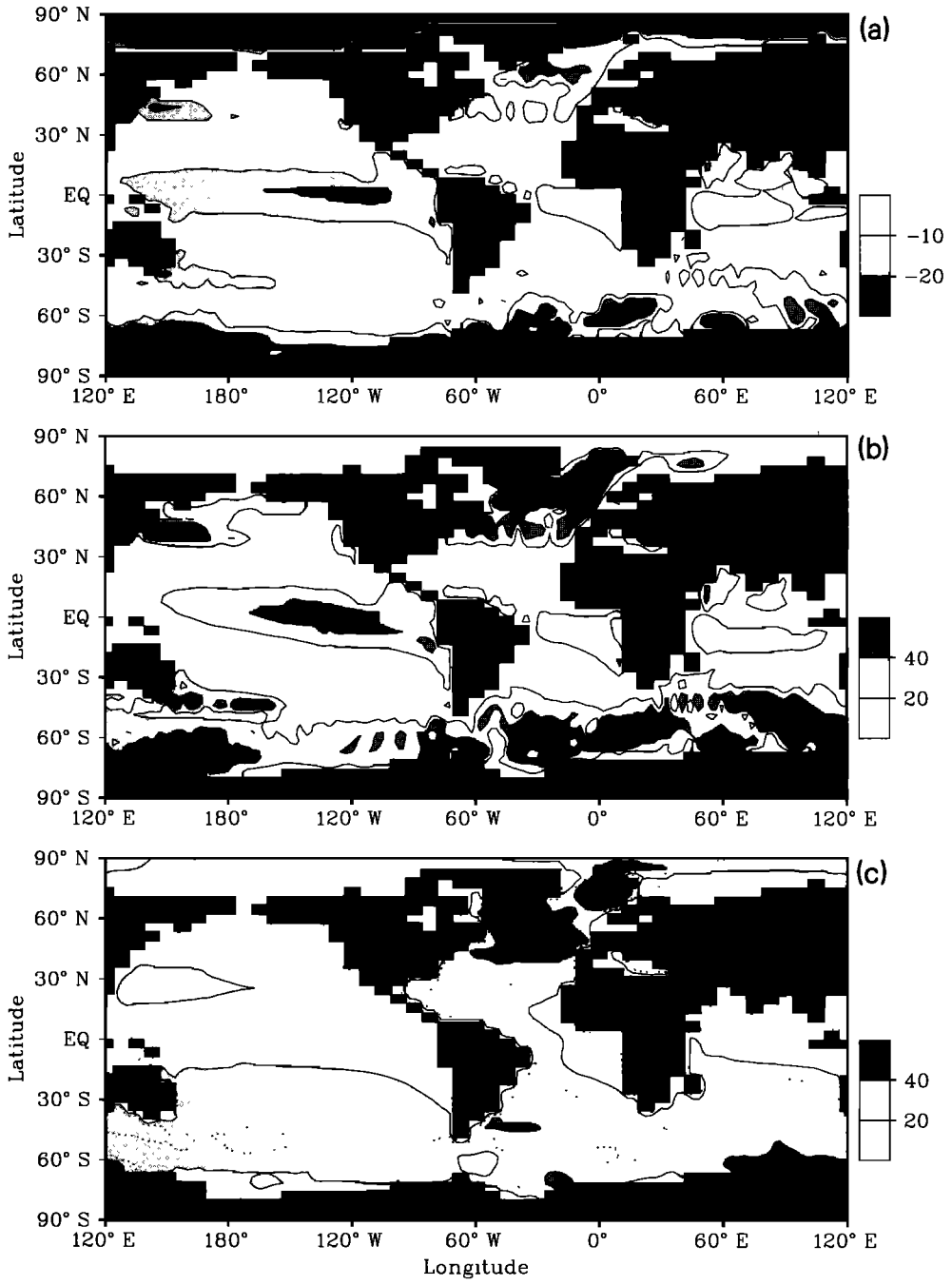

Fig. 4. (*a*) A map of the atmosphere-ocean difference, $\Delta\delta pCO_2$, for 1986 in ppm, from the standard simulation, A1.1. (*b*) and (*c*) Maps of the the cumulative input and standing crop in mol m^{-2}, respectively, from version A1.1.

pogenic input, $\Delta\delta pCO_2$, shown in Figures 2*a* and 4*a*. An interesting consequence of this is the following: the equatorial Pacific Ocean is known to be a source of CO_2 to the atmosphere, exhibiting high pCO_2 values [e.g., *Keeling*, 1968]. This is because the water that upwells there is rich in ΣCO_2 that has accumulated from regeneration of organic matter, and because the waters upwelling there are warmed. It is, however, a relatively strong net sink for anthropogenic CO_2 (Figures 2 and 4*b*) because the water that upwells at the equator has been out of contact with the atmosphere for a considerable amount of time and thus has only a small excess anthropogenic CO_2 load picked up when it was last in contact with the atmosphere (i.e., it has a relatively large negative value of $\Delta\delta pCO_2$). Thus the perturbation flux into these waters is large despite the fact that the gas exchange coefficient is small.

Of course, $\delta\Sigma CO_2$ does not simply stay in the region where it is added to the ocean, but is redistributed horizontally. We see from Figure 5 and by comparing Figures 4*b* with 4*c*, that $\delta\Sigma CO_2$ is lost from the equatorial regions and subpolar gyres, with the loss accumulating primarily in the subtropical gyres as well as some gain in the Arctic. This meridional redistribution is controlled predominantly by upwelling of waters with a small excess CO_2 load in the equatorial region and subpolar gyre, accompanied by Ekman transport towards and downwelling within the sub-

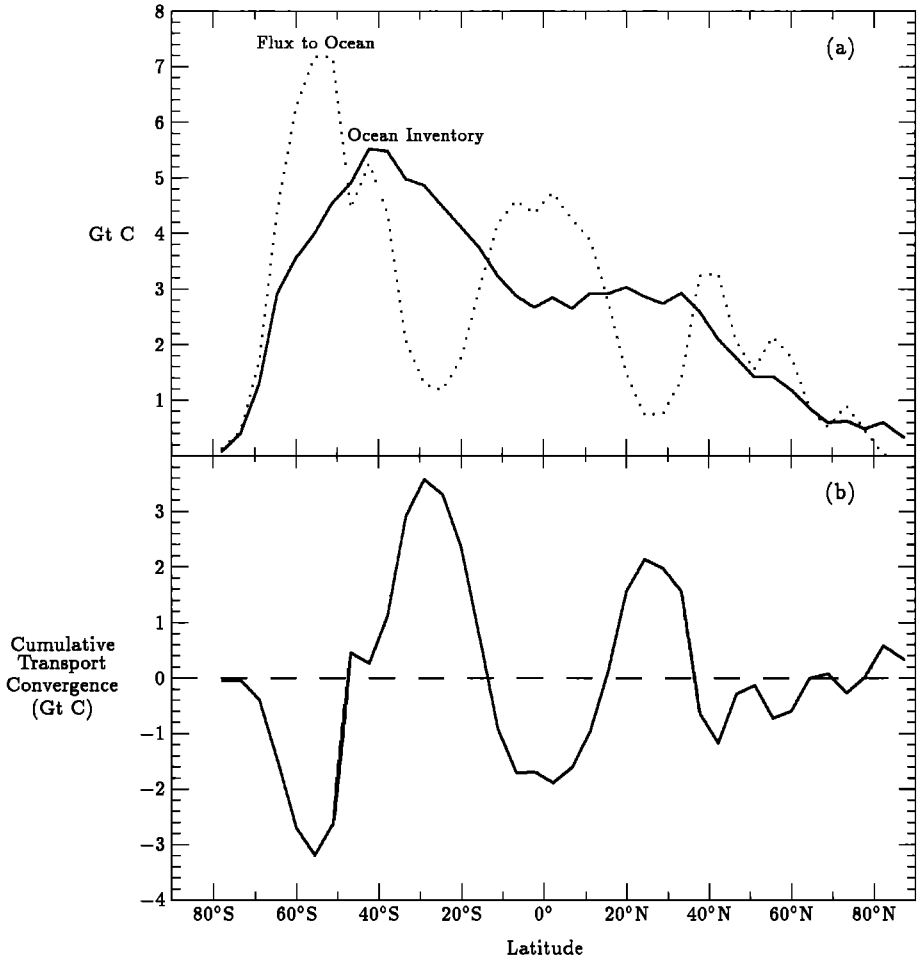

Fig. 5. (*a*) Zonal integral flux and standing crop in GtC per 4.5° latitude band in 1986 from model version A1.1. (*b*) Zonally integrated convergence of tracer in GtC per 4.5° latitude band resulting from transport from the beginning of the integration to 1986.

tropical gyre. Figure 6, which shows the zonally integrated meridional overturning, illustrates these circulation features. There is also a spreading of $\delta\Sigma CO_2$ from the region of greatest uptake in the eastern portion of the subtropical gyre to the western part. The circulation features that lead to these shifts have been dealt with in considerable detail in previous tracer modeling efforts such as those of *Sarmiento* [1983] and *Toggweiler et al.* [1989*a*], as well as discussions by *Broecker et al.* [1985*a*] of the bomb radiocarbon observations.

The tendency towards shallower penetration of $\delta\Sigma CO_2$ in the equatorial region and deeper penetration in the subtropics is clearly evident in the zonally averaged ocean basin profiles of Figure 7. The regions of deepest penetration are the North Atlantic deep water formation regions, and around the Southern Ocean in the Atlantic and Indian Oceans. The deeper penetration in the southern Indian Ocean region is probably not a realistic feature, as discussed by *Toggweiler et al.* [1989*b*].

3.2. *Comparison With Other Ocean Model Studies*

The box-diffusion and outcrop-diffusion models of *Siegenthaler and Oeschger* [1987] are representative of the types of box models that have been used to constrain the oceanic uptake estimates given in the *Houghton et al.* [1990] report (see Table 1). The only 3-D ocean general circulation model studies of oceanic uptake that have been carried out prior to ours are those of *Maier-Reimer and Hasselmann* [1987] and *Bacastow and Maier-Reimer* [1990], which were made using the Hamburg ocean model. Each of these previous studies will be discussed in turn.

Table 5 gives a comparison of our model with the bomb ^{14}C calibrated versions of the box models of *Siegenthaler and Oeschger* [1987]. The airborne fraction shown in Table 5*a* is the observed atmospheric inventory divided by the sum of the observed atmospheric inventory and the model-predicted oceanic CO_2 uptake. Table 5*b* shows the model-predicted atmospheric inventory divided by the total fossil CO_2 production which is used to force the model. The versions of the box-diffusion and outcrop-diffusion models which are forced with prescribed atmospheric CO_2 concentrations give airborne fractions of 0.581 and 0.479, respectively, for the period 1959 to 1983. Both are lower than the airborne fraction of 0.588 obtained by dividing the observed atmospheric increase by the estimated fossil CO_2 release. The box-diffusion and outcrop-diffusion models are thus able to account for the entire fossil CO_2 production and to take up a small additional amount of nonfossil production.

The airborne fraction over the same 1959 to 1983 time span for our standard simulation A1.1 is a relatively high 0.642, consistent with the results of Figure 1*b*, which show that our combined atmosphere-ocean uptake is smaller than the fossil CO_2 release. However, the total bomb radiocarbon uptake predicted with the on-line version of the ocean circulation model by *Toggweiler et al.* [1989*b*] at the time of

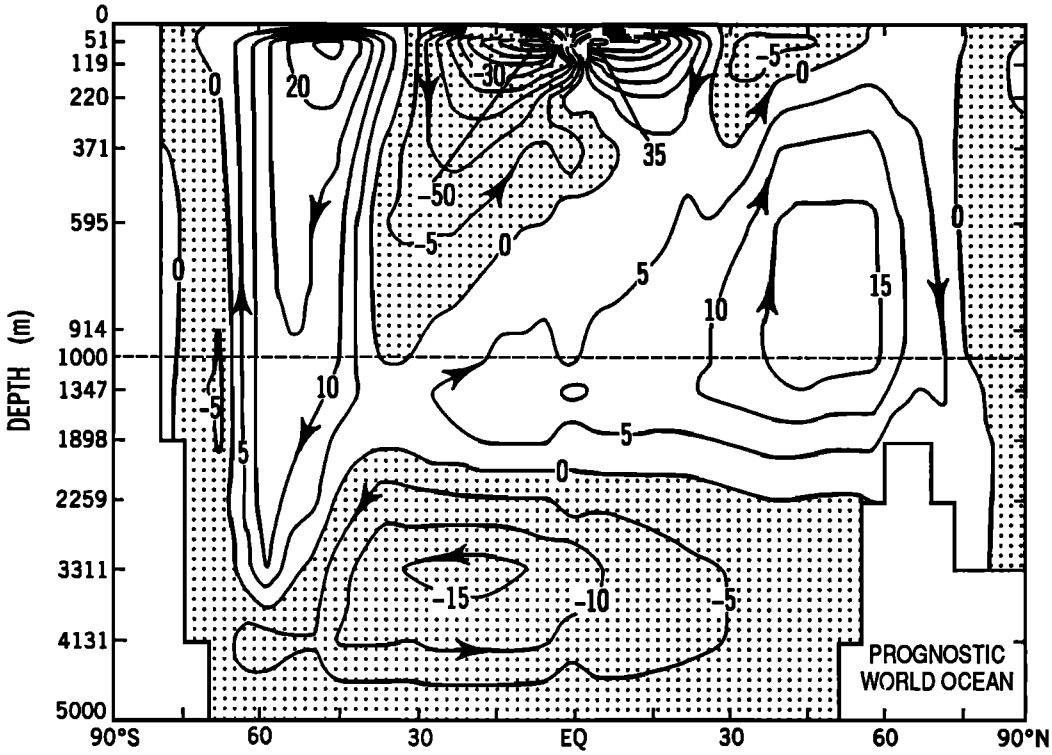

Fig. 6. The zonally integrated meridional overturning stream function from *Toggweiler et al.'s* [1989*a*] model P. Units are 10^6 m^3 s^{-1} (Sverdrups)

GEOSECS ($6.9x10^9$ atoms cm^2) is 16% lower than the estimate of $8.2x\ 10^9$ atoms cm^2 made by *Broecker et al.* [1985*a*] from GEOSECS observations. The off-line version of the model which we use gives a bomb radiocarbon uptake 6% lower than the observations. Part of the remaining difference can be compensated by increasing the gas exchange (recall from section 2.1 that our simulation has a gas exchange approximately 11% larger than the Toggweiler et al. study). However, as will be discussed in section 3.5, a better fit to the GEOSECS observations would also require a more rapid vertical exchange in the ocean. Furthermore, any modifications to the ocean circulation that would improve simulation of bomb radiocarbon uptake are also likely to reduce the airborne fraction. Thus we conclude that our oceanic uptake is most likely a lower limit.

The most convenient way to directly compare *Maier-Reimer and Hasselmann's* [1987] 3-D oceanic CO_2 uptake model with ours is through the Green's functions they calculated from simulations forced with a pulse in atmospheric CO_2. Table 5 shows a comparison of airborne fractions from Maier-Reimer and Hasselmann's Green's function with airborne fractions from a Green's function obtained from our 3-D model following the same procedure as Maier-Reimer and Hasselmann (see appendix for a more detailed description of the procedure). Both Green's functions calculations were forced by specifying the atmospheric concentration using the Siple ice core/Mauna Loa spline fit of Figure 1*a*. To the extent that the Green's functions are representative of the 3-D models, it appears that the Maier-Reimer and Hasselmann 3-D ocean model absorbs approximately 5% more CO_2 than our model A1.1.

The difference between *Maier-Reimer and Hasselmann's* [1987] model and ours becomes larger when differences in the gas exchange coefficient are considered. *Maier-Reimer and Hasselmann* [1987] use a spatially constant gas exchange coefficient equal to 0.050 mol $m^{-2}yr^{-1}ppm^{-1}$, 23% smaller than the global average of our wind-speed dependent coefficient, 0.065 mol $m^{-2}yr^{-1}ppm^{-1}$. In section 3.5 we present results showing that our standard A1.1 simulation gives a 7.0% higher CO_2 uptake than the same model using the Maier-Reimer and Hasselmann gas exchange coefficient. Adding the 7.0% difference attributable to gas exchange to the 5% difference obtained from the Green's function simulations, we find that the Maier-Reimer and Hasselmann 3-D ocean model takes up approximately 12% more CO_2 than our model, if both use the same gas exchange coefficient.

Figure 8 shows the air-sea difference, $\Delta\delta pCO_2$, calculated with our A1.1 standard simulation compared to the same property as simulated by *Maier-Reimer and Hasselmann* [1987]. The two maps are not directly comparable in that Maier-Reimer and Hasselmann force their model with the fossil CO_2 production summed to a deforestation source, whereas our model is forced with the atmospheric CO_2 concentration. In addition, their gas exchange coefficient is smaller. Nevertheless, one can gain some understanding into the differences between the models by a consideration of the figure. The larger oceanic uptake and lower gas exchange of the Maier-Reimer and Hasselmann model are reflected in the fact that their $\Delta\delta pCO_2$ (Figure 8*a*) is substantially larger than ours (Figure 8*b*). One possible reason for the difference in uptake is that our upper 51-m-thick layer is less than half the thickness of their 112-m-thick surface layer. In effect, their model has a 112-m-thick reservoir that is mixed infinitely fast, thus more effectively diluting any CO_2 that enters the ocean. Another effect of this thicker surface layer is that the Maier-Reimer and Hasselmann model must satisfy the Ekman divergence by upwelling water across the 112 m model level, whereas our model can use much shallower waters. For example, the total equatorial upwelling across 51 m in our model is 85 Sverdrups, (Sv), but it is only 55 Sv

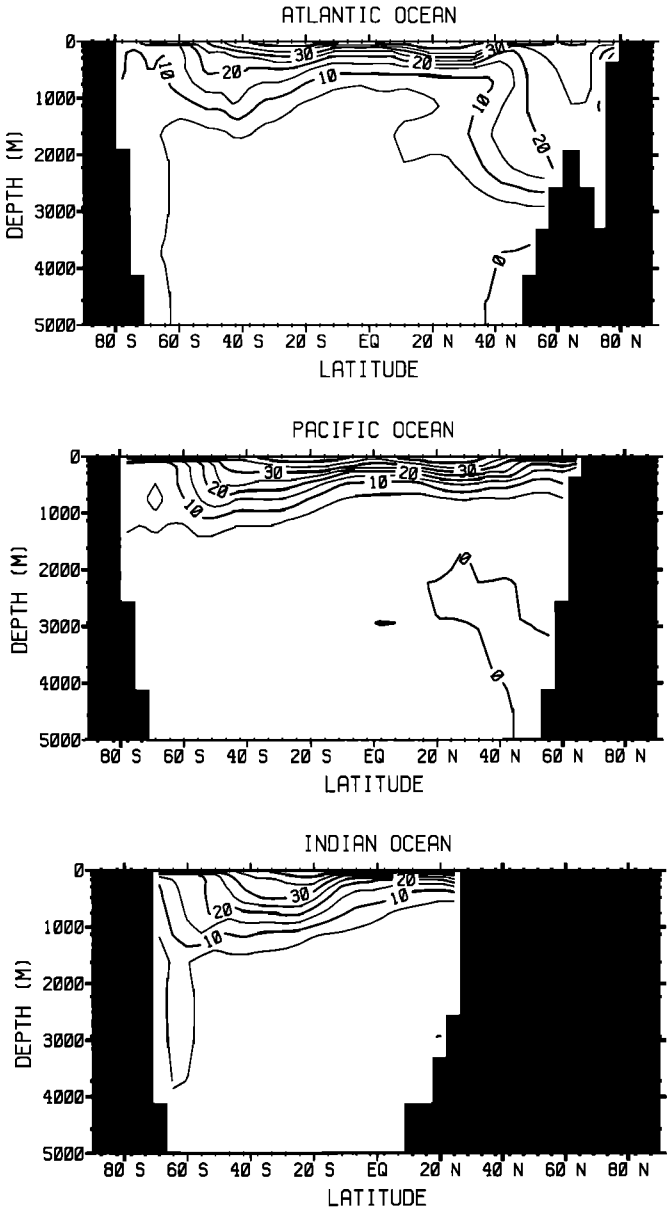

Fig. 7. Zonally averaged $\delta\Sigma CO_2$ in the Atlantic, Pacific, and Indian Oceans.

across 119 m (Figure 6); in Maier-Reimer and Hasselmann the total upwelling is of order 65 Sv at 112 m (their Figure 5). This stronger upwelling of somewhat deeper water enhances the air-sea difference by bringing up a larger amount of water that is less contaminated with fossil CO_2. Such an effect might help in particular to explain the higher $\Delta\delta pCO_2$ in the equatorial regions of Figure 8*a* than 8*b*.

Another reason for the difference between our simulation and that of *Maier-Reimer and Hasselmann* [1987] is the intense overturning in Maier-Reimer and Hasselmann's Southern Ocean. Their simulation of radiocarbon including the bomb component gives deep Southern Ocean concentrations which are higher than the observations and higher than *Toggweiler et al.'s* [1989*b*] simulation by more than 60 °/₀₀. These high Southern Ocean radiocarbon values lead to deep North Pacific radiocarbon values nearly as young as those of Toggweiler et al. even though the Pacific circulation is much slower in the Maier-Reimer and Hasselmann model, as evidenced by their north-south radiocarbon difference of over 120 °/₀₀. The north-south difference obtained by Toggweiler et al. is approximately 80 °/₀₀, in agreement with observations. The intense Southern Ocean overturning in the Hamburg model also explains why the North Atlantic radiocarbon age is significantly younger than Toggweiler et al.'s, even though the Hamburg model's deep water formation in the North Atlantic is too shallow.

This intense Southern Ocean overturning enhances the magnitude of the air-sea difference in the Southern Ocean and gives rise to a massive penetration of CO_2 in that region. This is clearly evident in Figure 9, which compares our simulation's $\delta\Sigma CO_2$ along GEOSECS tracks in the Western Atlantic and Pacific with that obtained by *Maier-Reimer and Hasselmann* [1987]. Except for the Southern Ocean, the Maier-Reimer and Hasselmann simulation is quite similar to ours. The greater penetration of $\delta\Sigma CO_2$ which Maier-Reimer and Hasselmann obtain at the southern end of the Western Atlantic and Western Pacific GEOSECS sections is also present in their radiocarbon simulation, which is not supported by the observations, as *Toggweiler et al.* [1989*b*] have pointed out.

Is the *Maier-Reimer and Hasselmann* [1987] model more realistic than ours? We believe from the comparison of

TABLE 5. Airborne Fraction

	A1.1	Box Diffusion	Outcrop Diffusion	A1.1 Green's Function	Hamburg Green's Function
(*a*) *Prescribed atmospheric* CO_2 *concentration* (*A*1.1)					
1770–1980	0.582	0.510	0.405	0.582	0.562
1959–1983	0.642	0.581	0.479	0.617	0.599
	A1.2	Box Diffusion	Outcrop Diffusion		
(*b*) *Prescribed fossil* CO_2 *production rate* (*A*1.2)					
1770–1980	0.638	0.612	0.519		
1959–1983	0.666	0.625	0.533		

The airborne fraction in Table 5*a* is defined as the ratio of the atmospheric increase to the increase in the atmosphere plus the ocean. In Table 5*b* the airborne fraction is the ratio of the atmospheric increase to the fossil production. See Table 4 and text for description of A1.1 and A1.2 simulations. The box-diffusion and outcrop-diffusion model results are from the bomb radiocarbon calibrated studies of *Siegenthaler and Oeschger* [1987]. We do not present the natural radiocarbon calibrated studies of Siegenthaler and Oeschger, as this calibration is more appropriate for longer time scale oceanic processes than the atmospheric CO_2 increase. "Hamburg" refers to the model of *Maier-Reimer and Hasselmann* [1987]. The A1.1 Green's Function and Hamburg Green's Function cases use the linear impulse response function approach described in the appendix and in Maier-Reimer and Hasselmann for an atmospheric pulse of 1.25x pre-industrial.

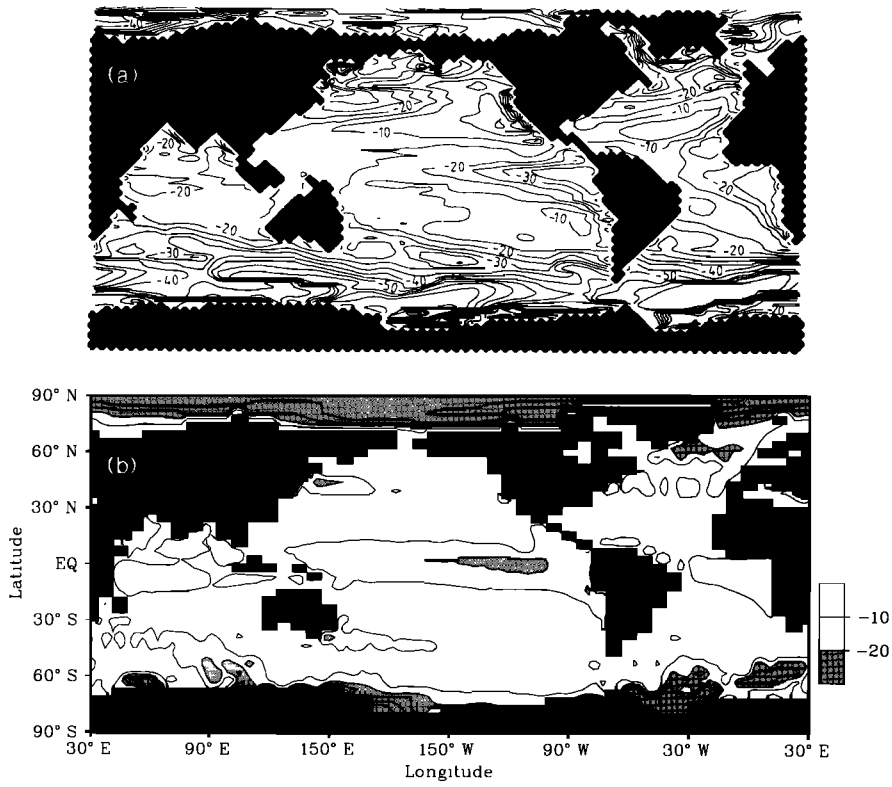

Fig. 8. (*a*) The 1984 air-sea difference, $\Delta\delta pCO_2$, calculated by *Maier-Reimer and Hasselmann* [1987] in the 112-m-thick upper layer of their model. This model is forced with the fossil fuel source, as is our simulation A2.1, but has added to it a source from land clearing. The gas exchange used is 0.05 mol m^{-2} yr^{-1} ppm^{-1}. (*b*) The 1986 $\Delta\delta pCO_2$ in the 51-m-thick upper layer of our standard version A1.1 model (see Table 8 for a description of the simulations). This model is forced with the observed atmospheric CO_2 partial pressure.

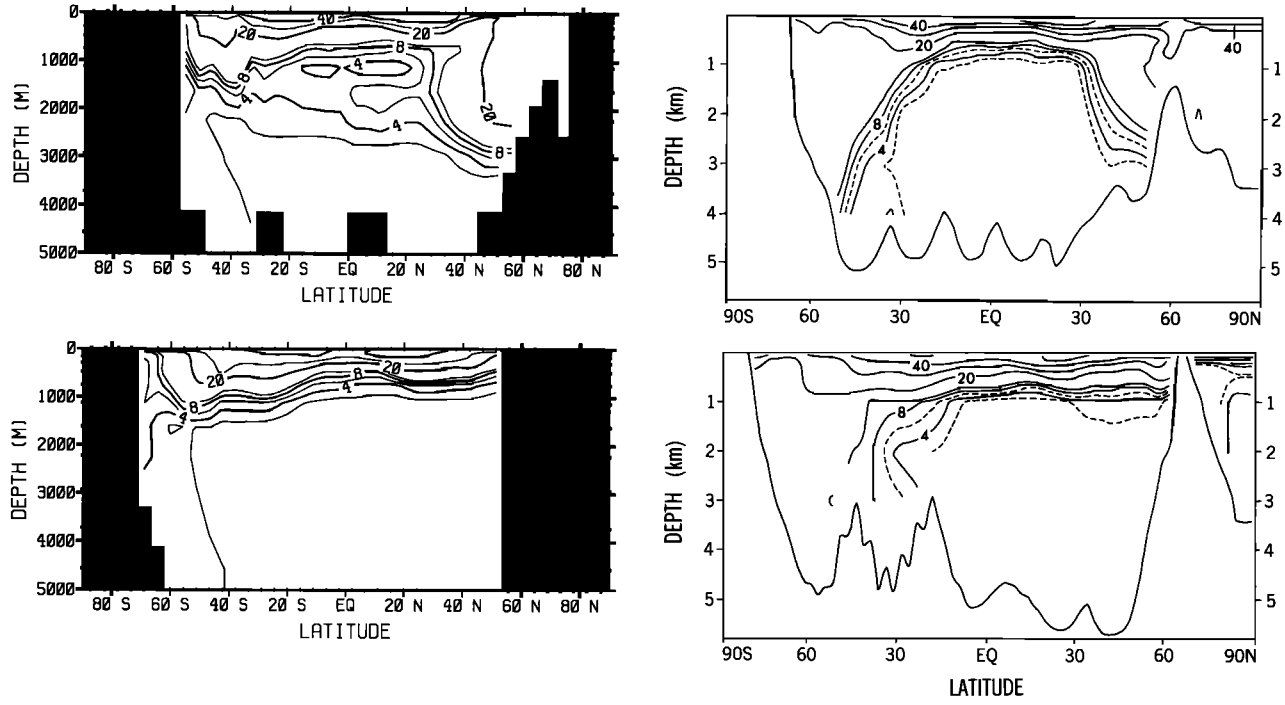

Fig. 9. Comparison of $\delta\Sigma CO_2$ along the GEOSECS tracks in the western Atlantic (upper panel) and western Pacific (lower panel) with the same quantity as calculated by *Maier-Reimer and Hasselmann* [1987] shown on the right.

our model radiocarbon simulation with the observations [*Toggweiler et al.*, 1989*b*] that our model does not have adequate exchange of surface with deep waters. The box-diffusion model, when calibrated with the bomb radiocarbon distribution, takes up significantly more CO_2 . The Maier-Reimer and Hasselmann model takes up an amount of CO_2 similar to that of the bomb-calibrated box-diffusion model, and is perhaps more realistic in this respect. How-

ever, the details of the Maier-Reimer and Hasselmann model suggest other types of problems. It appears that much of the additional uptake of CO_2 occurs in the Southern Ocean, which is not supported by either the comparison of their radiocarbon simulation with the observations [*Toggweiler et al.*, 1989*b*] or the comparison of their $\delta\Sigma CO_2$ simulation with data-based estimates (cf. section 3.3). We would therefore conclude that both models have significant difficulty in simulating penetration of perturbation CO_2 into the ocean correctly.

The comparison of these two models clearly illustrates the importance of good tracer data in model validation. No tracer is ideal, however. We note, in particular, that oceanic uptake of bomb radiocarbon is limited primarily by gas exchange (see discussion in section 3.5), whereas CO_2 uptake is controlled primarily by vertical exchange in the ocean (sections 3.1 and 3.5). The effect of this difference is clearly illustrated by comparison of Figures 10*a* with 10*b*. CO_2 uptake is strongly biased towards the Equatorial region and high latitudes, whereas bomb radiocarbon uptake by the oceans is much more evenly distributed and shows, in particular, far less input in the deep convection regions of the high southern hemisphere latitudes. It is thus important to study the possible impact of this difference in leading to erroneous estimates of CO_2 uptake with bomb radiocarbon calibrated box models. A three-dimensional model data set such as we have produced should make it possible to carry out such an analysis.

Bacastow and Maier-Reimer [1990] force their version of the Hamburg 3-D ocean model with a prescribed fossil CO_2

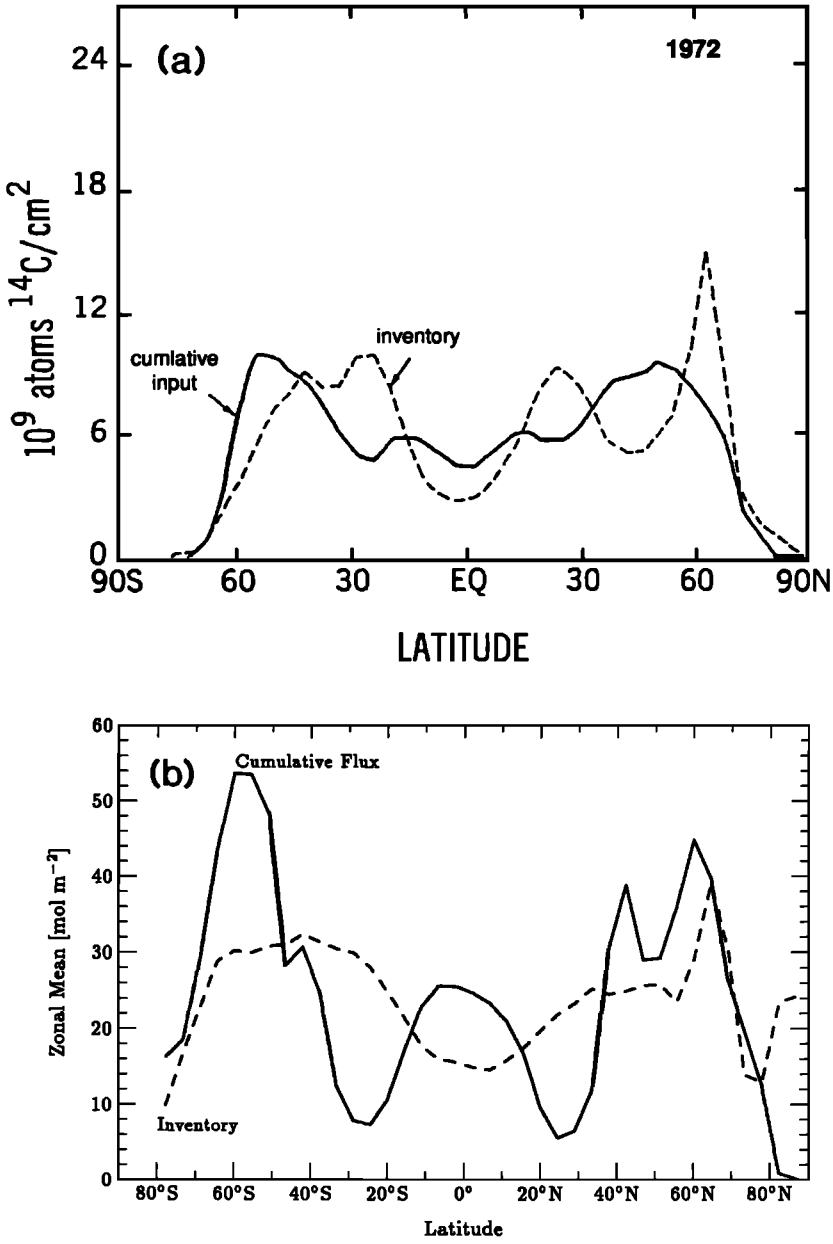

Fig. 10. (*a*) Cumulative bomb radiocarbon input and inventory in 1972 as predicted by *Toggweiler et al.* [1989*b*]. Toggweiler et al. give results for 1972 and 1990. We show the results for 1972 as being most representative of when the GEOSECS measurements were made. (*b*) Cumulative perturbation CO_2 flux into the ocean and inventory in 1986.

production rate, as do we in our simulation A1.2. They give an ocean-borne fraction (fraction of anthropogenic CO_2 which ends up in the ocean) of 0.32 for 1955–1975, approximately the same as the ocean-borne fraction of 0.328 calculated with our A1.2 simulation for the same period, which means that their model takes up less CO_2 than the *Maier-Reimer and Hasselmann* [1987] version of the Hamburg model. The difference between the two versions of the Hamburg model is due largely to a different parameterization of convective adjustment. Bacastow and Maier-Reimer show that the convective parameterization used by *Maier-Reimer and Hasselmann* [1987] increases the ocean-borne fraction by 0.03, i.e., 9%.

The results summarized in Table 5 also show that the ocean-borne fraction is always higher (i.e., the airborne fraction is always lower) in simulations forced by a prescribed atmospheric pCO_2 relative to those which prescribe a fossil CO_2 production rate. *Siegenthaler* [1986] explains this effect as resulting from the large early input of biospheric CO_2 implied by the ice core CO_2 data. As a consequence, the specific rate of increase of atmospheric CO_2 is slower in the model forced by a prescribed atmospheric CO_2 than in that forced by the fossil CO_2 production rate. The early biospheric input has more time to enter the ocean; thus the airborne fraction is lower when this early input is included. However, the effect is much larger in the box-diffusion and outcrop-diffusion models of *Siegenthaler and Oeschger* [1987] than in the 3-D model, indicating a different time dependence of the penetration of CO_2 into the ocean in the box-diffusion and outcrop-diffusion models as compared with the 3-D model. For the period 1959–1983, the difference between the airborne fraction of A1.1 and A1.2 is 0.024, compared with 0.044 and 0.054 for the box-diffusion and outcrop-diffusion models, respectively. Over the longer time span of 1770 to 1980, our models show a difference of 0.056 in the airborne fraction between the two simulations, whereas the box-diffusion model gives 0.102, and the outcrop-diffusion model gives 0.114.

The difference in behavior between the *Siegenthaler and Oeschger* [1987] models and our 3-D models results from the simplifications that were made in developing the box-diffusion and outcrop-diffusion models. It is well known that the box-diffusion and outcrop-diffusion models require higher diffusivities to simulate the bomb radiocarbon transient than to fit the natural radiocarbon distribution [e.g., *Siegenthaler*, 1983]. This is presumably because more rapid upper ocean processes dominate in the former case than the latter. A lower value for the diffusivity is needed to represent the long time scale processes important for natural radiocarbon as compared with the short time scale processes important for bomb radiocarbon. The rate of atmospheric CO_2 increase for simulations with prescribed atmospheric CO_2 concentration has a longer time scale than for simulations with prescribed fossil CO_2 production rate. Thus, the results of the radiocarbon simulations would suggest that the box-diffusion and outcrop-diffusion models should use a lower diffusivity in simulations with prescribed atmospheric CO_2 concentrations (longer time scale of CO_2 increase) than in those with prescribed fossil CO_2 production rate (shorter time scale). This would tend to bring the airborne fractions together. Our more realistic 3-D simulation does this. U. Siegenthaler and F. Joos (Studying anthropogenic CO_2 perturbations and oceanic tracers using a High-Latitude Exchange/Interior diffusion-advection (HILDA) ocean model, submitted to *Tellus*, 1991) have taken this into account in a new model by introducing a depth-dependent vertical diffusivity with high values in the top few hundred meters governing the uptake of anthropogenic CO_2 and bomb ^{14}C, and low values in the deeper levels which are important for predicting the distribution of natural ^{14}C. This new model is able to predict both the bomb and natural radiocarbon distributions with the same set of parameters.

3.3. *Comparison With Observations*

During development and analysis of this model, we have been concerned with finding ways of testing the model against observations. Thus, the comparison of radiocarbon predictions with observations carried out by *Toggweiler et al.* [1989*a*, *b*] is an important part of our long-term strategy to narrow the range of estimates for steady state model oceanic CO_2 uptake shown in Table 1. Unfortunately, the quality and number of oceanographic carbon system measurements are severely limited, both in terms of spacial resolution, and particularly as regards time evolution. In addition, it is very difficult, even under ideal circumstances, to infer from measurements the quantities $\delta\Sigma CO_2$ and $\delta pCO_{2_{OC}}$ which our model predicts. We explore, in the following discussion, the estimates for $\delta\Sigma CO_2$ and $\delta pCO_{2_{OC}}$ which are available; however, these estimates have provoked considerable controversy, so comparison with the model may be qualitative at best.

There have been a number of studies initiated by *Brewer* [1978] and *Chen and Millero* [1979] and continued by Chen and collaborators in a series of papers [*Chen and Pytkowicz*, 1979; *Chen*, 1982*a*, *b*; 1984; *Chen and Poisson*, 1984; *Chen et al.*, 1985, 1986; *Chen and Drake*, 1986] that have attempted to estimate $\delta\Sigma CO_2$ directly from ocean measurements. The ΣCO_2 concentrations are corrected for the addition of organic matter by using the apparent oxygen utilization (estimated by subtracting the observed oxygen from the saturation oxygen at the potential temperature of the water sample) times an appropriate Redfield ratio, and for the addition of $CaCO_3$ by using alkalinity. The quantity obtained by subtracting the estimated preformed ΣCO_2 from the corrected ΣCO_2 should then be $\delta\Sigma CO_2$. A critique of this work by *Shiller* [1981] raises serious questions regarding the role of mixing and its impact on the choice of end member water types to which *Chen et al.* [1982] respond (see also further response by *Shiller* [1982]). *Broecker et al.* [1985*b*] were also critical because of the large uncertainties involved in the many assumptions necessitated by this approach. On the other hand, the estimates of pre-industrial pCO_2 made by Chen and collaborators, e.g., the value of 268 $\pm$13 ppm reported on by Chen and Poisson, are lower than the ice core measurements of *Neftel et al.* [1985] and *Friedli et al.* [1986], by only $\sim$10 ppm, which is within the error of Chen and Poisson's estimate. Furthermore, the pattern of their estimated $\delta\Sigma CO_2$ is generally what one would expect from transient tracer observations. We therefore believe that a comparison with the model results is useful.

Figure 11 shows a comparison of model predicted $\delta\Sigma CO_2$ with estimates of this quantity by *Chen and Drake* [1986] along the GEOSECS Atlantic track, and along two north-south sections in the Pacific at 150°W and 165°E taken from *Chen et al.* [1986]. The model's inadequate penetration of

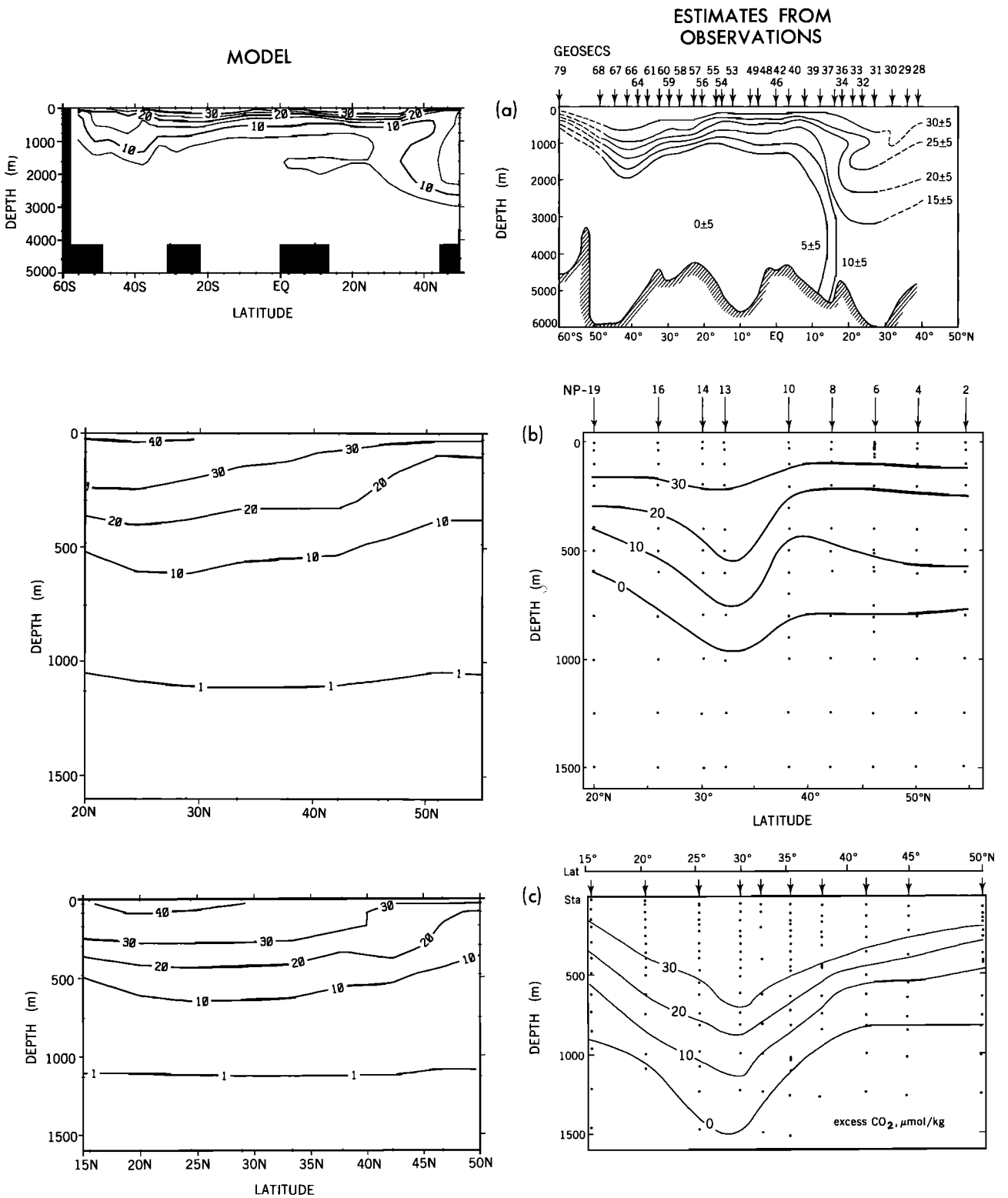

Fig. 11. Comparison of model calculated $\delta\Sigma CO_2$ with data-based estimates of the same quantity obtained as discussed in the text: (*a*) sections along the Western Atlantic GEOSECS track (data-based estimates on the right are from *Chen and Drake* [1986]), (*b*) sections along a north-south track at 150°W (data-based estimates on the right are from *Chen* et al. [1986]), and (*c*) sections along a north-south track at 165°E in the Pacific (data-based estimates on the right are from *Chen et al.* [1986]).

North Atlantic Deep Water as discussed by *Toggweiler et al.* [1989*a*] is clearly evident in the comparison of Figure 11*a* along the Atlantic GEOSECS track. The deep penetration of $\delta\Sigma CO_2$ in the Southern Ocean which *Maier-Reimer and Hasselmann* [1987] obtained in their model (Figure 9*b*) is not supported by the data based estimates of Figure 11*a*, which agree reasonably well with our model results.

The two North Pacific sections of *Chen et al.* [1986] (Figures 11*b* and 11*c*) show a penetration similar to that obtained by our model, although the structure is somewhat

different. These differences may reflect significant problems in the model's thermocline ventilation, but the errors in the data are too large for it to be worth studying them in detail. The task of validating the model thermocline ventilation is better left to comparisons of model predictions with bomb produced tritium observations [e.g., *Sarmiento*, 1983] or other tracers such as the chlorofluorocarbons.

The only attempt known to us to estimate the time evolution of oceanic pCO_2 is that of *Takahashi et al.* [1983] who give a figure summarizing the evolution of pCO_2 in the region of the Sargasso Sea based on 1959 International Geophysical Year (IGY) data, 1972 GEOSECS data, and 1982 Transient Tracers in the Ocean (TTO) data. Takahashi et al. obtained their estimate from a least squares linear fit to oceanic pCO_2 versus temperature for all data with temperatures greater than 10°C in the region 30°–40°N and 60°–80°W. The pCO_2 shown in Takahashi et al.'s figure is the mean obtained from the regression, which corresponds to a mean surface temperature of 19.6°C. Figure 12 shows a comparison of the annual mean of our model prediction with Takahashi et al.'s estimate. The model average is for the larger region 30°-50°N, 30°-80°W to allow sufficient model grid boxes (n=37) to perform the regression. The area used by Takahashi et al. could not be utilized here because only four model grid boxes are included and the annual mean temperatures do not include the 19.6°C average obtained by Takahashi et al. The slope of our model results is not as steep as the estimate of Takahashi et al., but it is difficult to put great confidence in the observational constraints, since spatial and seasonal resolution is limited.

The other data to which our model can be compared are estimates of oceanic uptake of CO_2 based on measurements of air-sea CO_2 difference. *Tans et al.* [1990] use such measurements to estimate an oceanic uptake of 1.88 GtC/yr for the period between 1972 and 1989 with a gas exchange coefficient that is comparable to the one we used in our model (Column A of Table 6). Our model gives an average uptake of 1.69 GtC/yr for the same period (Column B of Table 6), in good agreement with the data-based estimates. The geographic distribution of our perturbation uptake is, of course, different from the data-based air-sea CO_2 exchange estimate of Tans et al., because the latter includes an overlay of the pre-industrial fluxes. The dominant feature of the estimated pre-industrial fluxes obtained by taking the difference between our perturbation model and a normalized version of Tans et al.'s data-based estimate is a large outflow of +1.65 GtC/yr in the Equatorial band, balanced by an uptake of −1.74 GtC/yr in the southern hemisphere subtropics (Col-

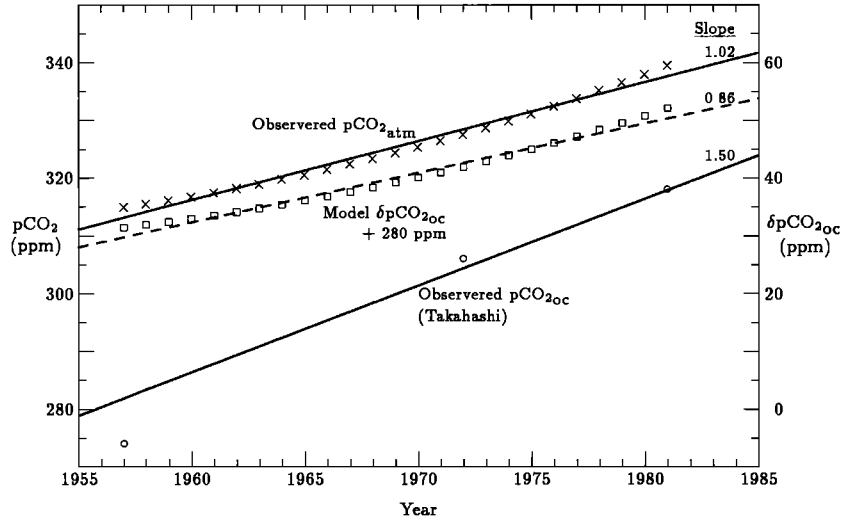

Fig. 12. Comparison of estimates of changes in oceanic pCO_2 through time by *Takahashi et al.* [1983] with model-predicted δpCO_2. The line through Takahashi et al.'s data is taken from his paper. His calculation gave low weight to the early estimate.

TABLE 6. Estimates of Pre-industrial Air-Sea Flux

Region	A Total Flux	B Anthropogenic CO_2 Uptake	C Pre-industrial CO_2 Flux	Region	D Pre-industrial CO_2 Flux
> 15°N	−0.59	−0.38	−0.15	> 15.6°N	−1.69
15°S–15°N	+1.30	−0.48	+1.65	15.6°S–15.6°N	+1.83
50°S–15°S	−2.39	−0.41	−1.74	39.1°S–15.6°S	−0.58
90°S–50°S	−0.20	−0.42	+0.24	90°S–39.1°S	+0.44
Total	−1.88	−1.69	0.00		0.00

All fluxes are given in GtC/yr with positive indicating a flux out of the ocean. Column A is the total flux as estimated from 1972–1989 ocean observations by *Tans et al.* [1990], including their correction of 0.37 GtC/yr to the Equatorial flux in order to account for the effect of El Niño. Column B is the 1972–1989 mean anthropogenic CO_2 uptake calculated by this study. Column C is the pre-industrial CO_2 flux estimated from (1.69/1.88) Col. A–Col. B . Column D is the pre-industrial CO_2 flux estimated by *Keeling et al.* [1989*b*] for 1984.

umn C of Table 6). However, a large southern hemisphere sink is inconsistent with results obtained from atmospheric models and data, as discussed in the following section.

3.4. *Comparison With Atmospheric Model Studies*

The large southern hemisphere oceanic sink which is suggested by data-based estimates such as those summarized in Column A of Table 6, requires a large interhemispheric CO_2 transport within the atmosphere from fossil CO_2 sources in the northern hemisphere, even after the geographical distribution of terrestrial biota sources and sinks is taken into consideration. Such a transport is not supported by 3-D atmospheric transport models constrained with the observed interhemispheric CO_2 gradient [*Tans et al.*, 1990](cf. also *Heimann et al.* [1986] and *Keeling et al.* [1989*b*] as well as 2-D studies by *Enting and Mansbridge* [1989], *Tans et al.* [1989], and references contained therein).

Tans et al. [1990] solve this difficulty in their scenarios 5 to 8 by ignoring the data-based southern hemisphere air-sea exchange flux estimates, while accepting those in the northern hemisphere (see Table 7), arguing that the former are rather poorly constrained by the data. These scenarios give a total oceanic uptake of only −0.3 to −0.8 GtC/yr for the period 1981–1987, leading them to conclude that the oceanic uptake is at most −1 GtC/yr. The remaining CO_2 is placed in the northern hemisphere temperate latitude terrestrial biota, with a resultant total net terrestrial sink of between −1.7 and −2.0 GtC/yr. This is in contrast to a net terrestrial sink of 0.0 GtC/yr obtained from Table 1 by summing the deforestation source of +1.6 GtC/yr to the missing sink of −1.6 GtC/yr, which we believe is due to uptake by terrestrial biota.

Keeling et al.'s [1989*b*] 3-D atmospheric CO_2 transport model is not able to support a large interhemispheric transport of CO_2 either. However, they solve the problem by putting a large flux of CO_2 into the northern hemisphere ocean (see Table 7) primarily by adjusting their preindustrial air-sea flux estimates (see Column D of Table 6). Their final scenario has a total oceanic uptake flux for 1984 of –2.30 GtC/yr, and net terrestrial sink of only –0.46 GtC/yr, both of which are close to the values in Table 1, and in good agreement with our ocean model results. Keeling et al. are also in agreement with Scenarios 1 and 2 of Tans et al., which are obtained by ignoring the data-based ocean CO_2 exchange measurements (see Table 7).

The *Keeling et al.* [1989*b*] scenario and *Tans et al.* [1990] Scenarios 1 and 2 have northern hemisphere oceanic CO_2 uptakes that are four times the data-based estimates (Table 7). Their southern hemisphere subtropical gyre uptakes are about half the data-based estimate. Could the data-based estimates be this far off? Tans et al. estimate the oceanic CO_2 uptake from $k_g \Delta pCO_2$, with ΔpCO_2 from maps made with measurements obtained during 1972–1989. Pacific equatorial measurements from the 1982–1983 and 1986–1987 El Niño periods are excluded. Their k_g has a global average value of 0.067 mol m^{-2} yr^{-1} ppm^{-1} using the winds of *Esbensen and Kushnir* [1981], and is in good agreement with our average of 0.065 mol m^{-2} yr^{-1} ppm^{-1}. However, the Tans et al. ΔpCO_2 data set has reasonably good coverage only in certain portions of the North Pacific and Atlantic, with relatively poor coverage elsewhere, particularly in the Southern Indian and Pacific Oceans. The uncertainty in the Tans et al. data-based flux estimate would obviously be quite large in the poorly sampled regions, but can it be so large in the North Atlantic and Pacific? As a measure of the difficulty, we note that Keeling et al.'s scenario has a 1980 air-sea CO_2 difference (ΔpCO_2) of −19 ppm in Pacific north of 15.6°N, as compared with +2 obtained from the observations by Tans et al. In the North Atlantic, *Keeling et al.* [1989*b*] obtain a ΔpCO_2 of −66 ppm north of 23.5°N, which is reduced to −52 ppm by inclusion of horizontal atmospheric diffusion and a wind speed dependent gas exchange. Tans et al.'s data-based estimate for the North Atlantic is −37 ppm north of 50°N, and −15 ppm between 15°N and 50°N.

The difference between the North Pacific and North Atlantic *Keeling et al.* [1989*b*] model estimates, and the observations of *Tans et al.* [1990], seem too large to explain as resulting from measurement uncertainty, although there is evidence which shows that temporal variability in oceanic pCO_2 is also large. *Watson et al.* [1991*b*] found a 1σ variability of about ± 10 ppm for several locations in the northeast Atlantic during the Joint Global Ocean Flux North Atlantic Bloom Experiment in 1989. *Wong and Chan* [1991] found that pCO_2 at Ocean Weather Station Papa in the North Pacific (50°N 145°W) varied between 290 and 340 ppm during the period 1973 to 1978. Watson et al. conclude that several tens of measurements would be needed at each location in order to define the atmospheric flux of CO_2 into the ocean to a small fraction of a gigaton. More measurements would help to resolve this issue. A most valuable contribution would be to obtain more detailed time series stations that would make it possible to develop a better understanding of the variability of air-sea fluxes and appropriate large scale sampling strategies.

One possible way of reconciling atmospheric modeling approaches, oceanic flux observations, and model-based oceanic anthropogenic CO_2 uptake estimates would be if

TABLE 7. Comparison of *Tans et al.* [1990] Air-Sea Fluxes With *Keeling et al.* [1989*b*]

Tans et al. [1990]				*Keeling et al.* [1989*b*]	
Region	Data	Scenarios 1 and 2	Scenarios 5 to 8	Region	Scenario
> 15°N	−0.6	−2.4	−0.6	> 15.6°N	−2.3
15°S–15°N	+1.6	+1.0	+1.3	15.6°S–15.6°N	+1.1
50°S–15°S	−2.4	−1.2	−1.7	39.1°S–15.6°S	−1.1
90°S–50°S	−0.2	+0.5	+0.5	90°S–39.1°S	+0.0
Total	−1.6	−2.1	−0.5		−2.3

Fluxes are given in GtC/yr with positive indicating a flux out of the ocean. The *Tans et al.* [1990] model results are averages for the scenarios indicated and correspond to the period 1980–1987. The data estimates are obtained from observations for the period 1972–1989. The *Keeling et al.* [1989*b*] results are taken from their Table 10 and correspond to May 15, 1984.

the atmospheric models have inadequate interhemispheric exchange. The study of *Tans et al.* [1990] makes use of the 3-D atmospheric tracer model developed at the Goddard Institute for Space Studies (GISS) for studies of CO_2 transport by *Fung et al.* [1987]. It was necessary to introduce horizontal diffusion to the model in order to simulate the interhemispheric transport of chlorofluorocarbons and ^{85}Kr [*Prather et al.*, 1987; *Jacob et al.*, 1987]. *Keeling et al.* [1989*b*] use the model developed by *Heimann and Keeling* [1989], which is also based on the GISS model, but with wind fields obtained from observations. This model also includes horizontal diffusion. The end result of these two approaches is similar, as a comparison of Tans et al.'s Scenarios 1 and 2 with Keeling et al.'s scenario shows (see Table 7). There may still be room for some uncertainty in the fact that the seasonal behavior of the interhemispheric gradient of chlorofluorocarbons and krypton-85 is very different from that of CO_2 . However, an ongoing study of the problem with a higher resolution atmospheric model at the Geophysical Fluid Dynamics Laboratory, which is able to fit chlorofluorocarbon-11 data reasonably well without any special adjustments, also gives a low interhemispheric transport of anthropogenic CO_2 (P. Kasibhatla, personal communication, 1991). In conclusion, we take as a working hypothesis that the atmospheric transport models are correct in their result that the total southern hemisphere oceanic CO_2 uptake cannot be as large as that obtained by the data-based air-sea exchange estimates of *Tans et al.* [1990]. We also take as a working hypothesis that the data-based North Atlantic and North Pacific air-sea exchange estimates obtained by Tans et al. are known sufficiently well to rule out the large northern hemisphere air-sea CO_2 uptake scenario of *Keeling et al.* [1989*b*]. Finally, we firmly believe that our oceanic uptake estimate of 1.9 GtC/yr represents a lower limit to the total uptake of anthropogenic CO_2 by the oceans. In the conclusion section we discuss possible ways of reconciling these conflicting results.

3.5. *Influence of Gas Exchange on CO_2 Uptake and Radiocarbon Model Validation*

There is considerable controversy over the magnitude of the gas exchange coefficient (e.g., compare the gas exchange rate of *Broecker et al.* [1985*a*], which we use, with that of *Liss and Merlivat* [1986] or *Watson et al.* [1991*a*]) so a series of simulations have been performed to examine sensitivity of the model results to gas exchange rate.

In simple 1-D ocean models, one finds that vertical mixing within the oceans, as opposed to gas exchange, is the rate limiting step for perturbation CO_2 uptake by the oceans [e.g., *Siegenthaler*, 1983]. As a result, the oceanic uptake of perturbation CO_2 is relatively insensitive to the gas exchange coefficient. However, there are many regions of the ocean, such as areas of strong upwelling and vertical convective overturning, where the extent of disequilibrium with atmospheric perturbation CO_2 will be significantly greater than that obtained by 1-D models. The flux of perturbation CO_2 into the ocean in such regions should show more sensitivity to the gas exchange coefficient than that shown by 1-D models [e.g., *Memery and Merlivat*, 1985]. Thus, a detailed sensitivity study of the 3-D simulation results is necessary. We have performed several such studies, summarized in Table 8. We discuss in greatest detail the simulation in which the gas exchange coefficient was doubled (A3.1) over the standard simulation.

The regions of the model ocean which are well out of equilibrium with the atmospheric fossil CO_2 perturbation can be seen in Figures 2*a* and 4*a*. Note that the air-sea pCO_2 difference, $\Delta\delta pCO_2$, shown in the figures is the difference between the perturbations in ocean and atmosphere, as defined in Table 2. It should not be confused with the difference between the absolute partial pressures, ΔpCO_2, that drives the total local exchange flux. The high correlation of these regions with areas of strong upwelling (particularly along the equator) and with areas of convective overturning (particularly in high latitude deep water formation regions) can be clearly seen by comparing Figure 4*a* with Figure 3. A doubling of the gas exchange coefficient significantly increases the flux into the ocean in these regions, as would be expected (Figure 13*a*). However, the increase in the flux is much less than the factor of two increase in the gas exchange coefficient. This is because the larger flux of perturbation CO_2 into the ocean attributable to more intense gas exchange adds CO_2 to the surface at a rate faster than it can be transported to depth. The surface CO_2 concentration therefore increases (Figure 13*b*), reducing the air-sea pCO_2 difference and thus the flux.

Despite the larger fluxes in some regions of the doubled gas exchange rate simulation (A3.1), the overall effect upon total model inventory is small (Table 8) because the area of these regions is relatively small, and because almost the entire subtropical region is either unchanged or actually has a reduced flux (see Figure 13*a*). The reduced CO_2 flux in the subtropics is explained by the nature of the supply of

TABLE 8. Sensitivity of CO_2 Uptake to Gas Exchange Coefficient in Simulations With Prescribed Atmospheric CO_2 Concentration

Simulation	$\bar{k}_g^{ave*}$ mol m^2 yr ppm	$\bar{k}_g^{ave*}$ Normalized to A1.1	Oceanic Uptake (1750–1986) Gt C	Oceanic Uptake (1750–1986) Normalized to A1.1
Simulations Using Esbensen and Kushnir [1981] *Winds*				
A1.1 (standard)	0.065	1.00	100.6	1.000
A2.1 (k_g = 1.2x standard)	0.078	1.20	103.1	1.025
A3.1 (k_g = 2.0x standard)	0.130	2.00	109.8	1.091
A5.1 (k_g from *Liss and Merlivat* [1986])	0.029	0.55	89.1	0.886
Simulations Using a Spatially Constant Gas Exchange				
A4.1 (standard)	0.065	1.00	98.0	0.974
A6.1 (same as *Maier-Reimer and Hasselmann* [1987])	0.050	0.77	94.0	0.934

*Here, $\bar{k}_g^{ave}$ is the average over ice-free ocean.

surface waters to the subtropics, where downwelling predominates (see Figures 3*a* and 6), which is primarily convergent Ekman transport from regions of upwelling in the subpolar region and at the Equator (see Figure 6). The increased gas exchange in simulation A3.1 leads to a more efficient perturbation CO_2 invasion into the upwelling waters within the subpolar and Equatorial regions, so that by the time these waters arrive in the subtropics, they have less capacity to absorb CO_2 than in simulation A1.1.

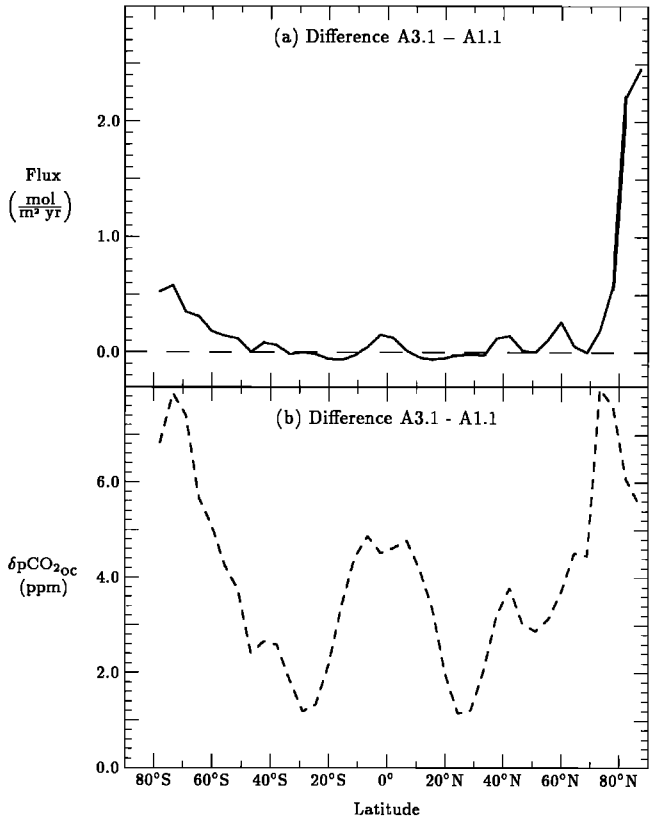

Fig. 13. Difference between the (*a*) zonal mean annual flux and (*b*) δpCO_2 of simulation with the doubled gas exchange rate case, version A3.1, and A1.1 (A3.1 – A1.1).

Table 8 and Figure 14 summarize the results of a further series of studies that were carried out to examine the sensitivity of the perturbation CO_2 uptake to the magnitude of the gas exchange. Simulations A2.1 and A3.1, with an increase of 20% and 100% in the gas exchange coefficient over our standard A1.1 simulation, give an increase of only 2.5% and 9.2%, respectively, in the cumulative CO_2 uptake to 1986. Simulation A5.1 was carried out in order to study how the CO_2 uptake would be affected by the *Liss and Merlivat* [1986] gas exchange coefficient formulation. It has an average gas exchange coefficient which is 45% of that in A1.1, and a cumulative uptake which is lower than that of A1.1 by 11.4%. The summary in Figure 14 suggests that the sensitivity of perturbation CO_2 uptake to gas exchange increases at lower gas exchange coefficients. Such a result would be as expected: with lower gas exchange coefficients, the vertical overturning in the model will become less dominant as the factor limiting uptake and there should be more sensitivity to the gas exchange coefficient.

A measure of the sensitivity of the perturbation CO_2 flux to the structure of the wind speed dependence of the gas exchange coefficient formulation can be obtained by comparing Simulation A4.1 with A1.1. Simulation A4.1 has a spatially constant gas exchange coefficient equal to the area weighted average of A1.1 (0.065 mol m^{-2} yr^{-1} ppm^{-1}). The uptake is 2.6% lower than A1.1, showing only a modest sensitivity to the difference in pattern between these two cases. This somewhat unexpected finding is partly a result of opposing effects (see Figures 2*a* and 2*b*): near 60°N and 60°S the higher than average k_g leads to a larger uptake in simulation A1.1 than in A4.1, but in the equatorial region, with its low wind speeds, the situation is reversed. Simulation A6.1 uses the same gas exchange coefficient as the *Maier-Reimer and Hasselmann* [1987] study: a spatially constant value of

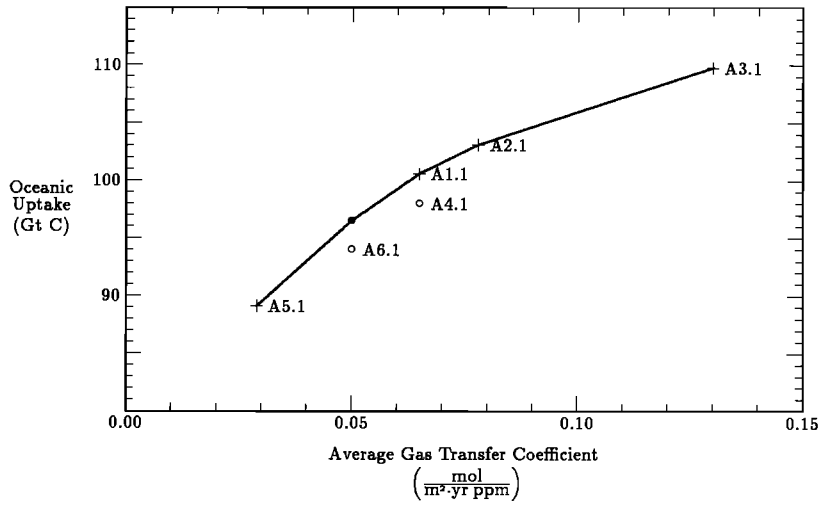

Fig. 14. Oceanic uptake of CO_2 versus global average gas exchange coefficient over ice-free ocean for various model simulations (see Table 8). Models A1.1 (the standard case), A2.1, A3.1, and A5.1, indicated by crosses, all have wind speed dependent gas exchange using *Esbensen and Kushnir*'s [1981] data. A smoothed line is drawn through these results. Models A4.1 and A6.1, indicated by open circles, use constant gas exchange coefficients. Note that model A4.1, which uses a constant gas exchange coefficient equal to the global average of A1.1, has a lower CO_2 uptake than A1.1. The solid circle gives model result A6.1 as adjusted by the fractional difference between A4.1 and A1.1.

0.050 mol m^{-2} yr^{-1} ppm^{-1}. Figure 14 shows that the cumulative CO_2 uptake predicted by A6.1, when increased by the 2.6% difference between A4.1 and A1.1, falls on the line drawn between other model results which used a wind speed dependent gas exchange coefficient formulation.

The 3-D results thus confirm the simple 1-D models results showing very low sensitivity of perturbation CO_2 uptake to gas exchange. The CO_2 flux is relatively sensitive to the gas exchange coefficient in regions of strong vertical exchange, but the overall impact of these regions is small. This is partly because the area of these regions is small, and partly because the perturbation CO_2 flux in areas of weak vertical exchange in the subtropics responds in the opposite direction. Taken over the ocean as a whole, vertical exchange is the dominant process in limiting perturbation CO_2 flux into the ocean. However, it remains to be seen if low sensitivity will still be exhibited by models which include the seasonally varying mixed layer depth, the effect of seasonal changes in gas exchange coefficient, and the effect of seasonal changes on CO_2 solubility (which affects the air-sea difference,$\Delta\delta pCO_2$, for a given $\delta\Sigma CO_2$)

Both *Monfray et al.* [1989] and *Bacastow and Maier-Reimer* [1990] employed the 3-D Hamburg ocean model and found the same low sensitivity of oceanic CO_2 uptake to gas exchange. Bacastow and Maier-Reimer's study of the effect of a doubled gas exchange gives an increase in oceanic CO_2 uptake of 5.0% for the period 1955–1975 (their ocean-borne fraction increases by 0.016 compared with their standard case result of 0.32). Their 5.0% increase is comparable to our 5.9% increase obtained for the same period (an ocean-borne fraction of 0.373 for our standard case versus 0.395 for the doubled gas exchange case). The small difference between these results is probably due to some combination of the difference in the forcing functions and the difference in k_g. That is, Bacastow and Maier-Reimer force their model with fossil CO_2 production and a constant k_g; we force ours with observed atmospheric CO_2 and wind-speed dependent k_g.

Unlike CO_2, radiocarbon uptake by the oceans is relatively sensitive to the gas exchange coefficient because it takes ~10 times longer for the surface concentration of radiocarbon to equilibrate with the atmosphere than it does for CO_2 [*Broecker and Peng*, 1982]. In the case of CO_2 , the surface concentration adjusts quickly to an increased gas exchange coefficient by reducing the air-sea CO_2 difference so that the net flux of CO_2 increases only moderately. In the case of radiocarbon the surface concentration adjusts by only a small amount, so that the net flux changes nearly in direct proportion to the changes in the gas exchange coefficient. Thus, simulation P′ of *Toggweiler et al.* [1989*b*], which has a 20% higher gas exchange than their simulation P, predicts a greatly improved bomb radiocarbon inventory which is lower than the observations by less than 4% as compared to 16% for P. However, this improvement is associated with surface radiocarbon concentrations that are higher than observations. One might therefore conclude that an improved bomb radiocarbon uptake model will require both more intense gas exchange (to increase the flux into the ocean) and more intense surface to deep ocean exchange (to reduce the surface concentration). An increased surface to deep ocean exchange, the need for which is suggested by the foregoing discussion, would increase the CO_2 uptake significantly.

There is a difficulty with this interpretation, however. The gas exchange coefficient used by *Toggweiler et al.* [1989*a*, *b*] is the natural and bomb radiocarbon based wind speed dependent formulation of *Broecker et al.* [1985*a*] which we use here. This formulation gives a global average CO_2 gas exchange of 0.065 mol m^{-2} yr^{-1} ppm^{-1} with the vector-averaged annual mean wind speeds of *Esbensen and Kushnir* [1981]. The gas exchange coefficient formulation of *Liss and Merlivat* [1986] gives a global average CO_2 gas exchange of only 0.029 mol m^{-2} yr^{-1} ppm^{-1} with the same winds. If the latter formulation is closer to reality, it will be difficult, if not impossible, to reconcile radiocarbon model predictions with oceanic observations.

One avenue of research that is being undertaken to resolve this issue is to attempt new analyses of wind speeds, for example, by using satellite scatterometer measurements and including temporal variability. A recent overview by *Etcheto and Merlivat* [1988] gives a range of global gas exchange coefficients of 0.029 to 0.042 mol m^{-2} yr^{-1} ppm^{-1} (*Thomas et al.* [1988] and *Monfray* [1987], respectively) resulting from the *Liss and Merlivat* [1986] gas exchange coefficient formulation using different wind speed data sets (cf. also *Erickson* [1989] and *Heimann and Monfray* [1989]). However, even the highest wind speeds from these results are significantly lower than what the radiocarbon observations require. It has been suggested that CO_2 gas exchange may be enhanced by carbonic anhydrase catalysis, but evidence for this has yet to be found in the oceans [*Goldman and Dennett*, 1983].

Studies which show promise of resolving the inconsistency between the Liss and Merlivat gas exchange rate and the radiocarbon results are those which give evidence suggesting that the Liss and Merlivat function may indeed be too low. *Wanninkhof* [1992] shows new evidence for the importance of fetch in determining the gas exchange rate and suggests that the low gas exchange rate of Liss and Merlivat is based on fetch limited studies. On the other hand, the open ocean results of *Watson et al.* [1991] agree with the Liss and Merlivat function. The study of *Spitzer and Jenkins* [1989] suggests an important role for bubble injection at lower wind speeds than Liss and Merlivat, with overall gas exchange rates that are higher than those of Liss and Merlivat. To resolve the discrepancy between gas exchange rates and radiocarbon results requires not only further studies of gas exchange, but also better observational constraints on surface radiocarbon concentrations and bomb radiocarbon inventories so that these can be determined as accurately as possible.

4. CONCLUSIONS

Our simulation of fossil CO_2 uptake makes use of a simplified model of ocean chemistry based on approximating surface ocean properties with a constant salinity and alkalinity, and with a pre-anthropogenic surface ΣCO_2 that is taken to be in equilibrium with an atmospheric CO_2 of 280 ppm everywhere. Our perturbation model does not include biological fluxes and assumes that these have been unchanged since pre-industrial time. When forced with the Siple ice core/Mauna Loa atmospheric pCO_2 record of Figure 1*a*, the combined observed atmospheric uptake and modeled oceanic uptake of CO_2 between 1958 and 1986 (excluding other sinks) is 9.6% less than the estimated fossil fuel CO_2 emission. A net emission from terrestrial vegetation sources, such as very likely exists, would make this "missing sink" even larger.

One of the most important problems of carbon cycle research is to determine where all the additional CO_2 is going.

Models of the ocean place strong constraints on what processes are important in determining the oceanic sink. Starting at the surface of the ocean, the results of this study confirm earlier work with simpler models showing that the magnitude of the gas exchange coefficient is not an important factor in model estimates of CO_2 uptake. Simulations with variations in the gas exchange coefficient of order 100% lead to substantial local modifications in the CO_2 uptake, but the global impact is only of order 10%. Still, the model described here is based on mean annual conditions and does not take into account seasonal processes that may be of importance. However, based on the low sensitivity shown by our gas exchange experiments, the inclusion of seasonality probably will not affect the results significantly except locally. To test this, simulations with seasonal models are now being prepared. It should be noted that, although a better knowledge of the gas exchange coefficient will not have a significant impact on model simulations, it is of critical importance to estimates of CO_2 flux from direct measurements of the air-sea CO_2 difference, since the flux estimated this way is directly proportional to the magnitude of the gas exchange coefficient.

Our parameterization of ocean chemistry is highly simplified, and it does not take into consideration new results by *Goyet and Poisson* [1989] suggesting that the carbonic acid dissociation constants used in our work may be incorrect. A more realistic parameterization of the ocean chemistry will give slightly different relationships between the perturbation in the partial pressure of CO_2 and that in total carbon (the buffer factor). The carbonic acid dissociation constants of Goyet and Poisson give moderately higher buffer factors at lower temperatures. Carbon cycle models need to be developed which solve for the actual total carbon and alkalinity fields, such as those of *Maier-Reimer and Hasselmann* [1987] and *Bacastow and Maier-Reimer* [1990]. However, the comparison of our model results with these studies, and some preliminary calculations with the Goyet and Poisson dissociation constants, suggest that neither of these changes is likely to have a large effect on simulated CO_2 uptake by the ocean.

We come, now, to the ocean circulation. The bomb radiocarbon simulation of *Toggweiler et al.* [1989*b*], which used the on-line version of our ocean circulation model, underpredicts the estimated GEOSECS inventory by 16% , which is only partially compensated for in the off-line version. The Toggweiler et al. sensitivity study discussed in section 3.5 suggests that an increase of the surface to deep exchange will be required to improve the radiocarbon simulation. An increased vertical exchange will also increase the CO_2 uptake, since it is clear from our simulations with different gas exchange coefficients that gas exchange is not limiting CO_2 uptake. One modification to the model that has been shown to give an enhancement of vertical exchange is to orient the mixing tensor along isopycnal surfaces (K. Dixon, personal communication, 1991). Seasonal forcing also needs to be included, although recent simulations suggest that the impact of this on tracer uptake is surprisingly small (J. R. Toggweiler, personal communication, 1991).

We conclude, from the underestimate of the bomb radiocarbon uptake, in the on-line version of our model, which is only partially compensated for in the off-line version, that our simulation most likely provides a lower limit to anthropogenic CO_2 uptake by the ocean if the background carbon cycle is in steady state. Our value of 1.9 GtC/yr for 1980 to 1989 is close to the IPCC assessment average of 2.0 GtC/yr given in Table 1 [*Houghton et al.*, 1990]. However, it is inconsistent with the uptake estimate of *Tans et al.* [1990] which they obtain with an atmospheric model constrained with atmospheric data, from which they conclude that the oceanic uptake must occur primarily in the northern hemisphere. Based on this constraint, combined with data-based estimates of air-sea exchange, they suggest that oceanic uptake is less than 1 GtC/yr. Our ocean model strongly supports the high oceanic CO_2 uptake scenario. It is difficult to see how one can make reasonable predictions of the oceanic bomb radiocarbon uptake without also obtaining a perturbation CO_2 uptake of order 2 GtC/yr. One possible way of reconciling these results is if there has been an alteration in the natural cycling of carbon in the ocean. A reduction of oceanic uptake of CO_2 would require a reduction in the export of organic or inorganic carbon to the abyss by a change in the behavior of ocean biology or the circulation between the period when the bomb radiocarbon measurements were made in the early 1970's , and the 1980–1987 time span considered by Tans et al. It is the possibility that these processes might play a significant role in the future behavior of the ocean carbon cycle, or that they may already be playing a role, that has led us to begin the development of models of ocean biology [*Sarmiento et al.*, 1989]. On the other hand, the pre-industrial South Pole ice core data of *Siegenthaler et al.* [1988], with its modest fluctuations of order $\pm$ 5 ppm over 1000 years, suggest to us that is unlikely that ocean biology or circulation could be making such a large difference.

Another way of reconciling high oceanic anthropogenic CO_2 uptake estimates obtained by ocean circulation models with low uptake estimate of *Tans et al.* [1990], is if a substantial portion of the uptake occurs by river transport into the northern hemisphere ocean. The Tans et al. constraint on northern hemisphere oceanic uptake is based on their air-sea exchange estimates. Such estimates would not take into account transport by rivers. J. L. Sarmiento and E. Sundquist (Oceanic uptake of anthropogenic CO_2: A new budget, submitted to *Nature*, 1991) conclude that river transport may indeed be significant, although it is not sufficient to explain all of the discrepancy. Further progress on this problem is going to require improved spatial and temporal resolution of measurements of the air-sea CO_2 difference, as well as an improved understanding of the gas exchange coefficient.

The atmospheric transport models in *Tans et al.* [1990] and *Keeling et al.* [1989*b*] also require a small southern hemisphere oceanic sink. This implies that the pre-industrial air-sea CO_2 flux, which we did not predict in our study, must have had a large southern hemisphere source and northern hemisphere sink such as that in Keeling et al.'s scenario shown in Column D of Table 6. This would have required a southward transport in the ocean, evidence for which should still exist [*Brewer et al.*, 1989; W. S. Broecker and T. H. Peng, Interhemispheric transport of CO_2 by the great ocean conveyor, submitted to *Nature*, 1991].

APPENDIX

We have carried out a series of simulations of the oceanic response to pulse inputs of atmospheric CO_2 at time 0 of 0.25x, 1x, and 3x the pre-industrial pCO_2 of 280 ppm. *Maier-Reimer and Hasselmann* [1987] show that the results

TABLE A1. Coeffiecients for Exponential Fits to the Atmospheric Response to a Pulse Input

Initial Input	A_0	A_1	τ_1, years	A_2	τ_2, years	A_3	τ_3, years	A_4	τ_4, years
0.25	0.164	0.245	358.8	0.302	60.8	0.229	10.3	0.059	1.0
1.00	0.174	0.275	376.6	0.307	67.7	0.189	10.7	0.054	0.9
3.00	0.208	0.358	433.3	0.261	83.9	0.131	11.2	0.042	0.8

The numbers given in the initial input column are the fraction by which the atmospheric pCO_2 was increased above its pre-industrial value of 280 ppm.

from such simulations can be usefully represented as a linear impulse response Green's function consisting of a superposition of exponentials

$$G(t) = A_0 + \sum_j A_j exp(-t/\tau_j)$$

The atmospheric CO_2 signal $y(t)$ can then be given as a function of an arbitrary emission function $x(t)$. If the time span t is broken down into n finite intervals, we have

$$y(n) = \sum_{i=1}^{n} G(i) \times (n-i)$$

$y(t)$ and $x(t)$ have units of atmospheric concentration (GtC or ppm). One can also use this approach to deconvolve the source function $x(t)$ from the observed atmospheric CO_2 signal $y(t)$. Noting that $G(1) = 1$, we have for the deconvolution

$$x(n) = y(n) - \sum_{i=2}^{n} G(i) \times (n-i)$$

The value of this approach has been further demonstrated by *Harvey* [1989], who has used the functions given by Maier-Reimer and Hasselmann in his study of scenarios for the management of CO_2 . Table A1 summarizes the A_j and τ_j coefficients we obtain from our study and which are used in generating the results shown in Table 5.

Acknowledgments. J. Sarmiento appreciates the long-standing support provided by GFDL/NOAA, in particular, from K. Bryan and J. Mahlman. U. Siegenthaler acknowledges the support of H. Oeschger for his research. We have profited greatly from extensive interactions with J. R. Toggweiler and T. Takahashi, whose input we much appreciate. R. Najjar, R. Slater, K. Dixon, and M. Cox lent valuable expertise to the modeling effort. Reviews by C. D. Keeling, H. Levy, S. Manabe, and J. R. Toggweiler helped improve the paper significantly. J. Olszewski assisted in preparation of the manuscript and figures. Financial support has been provided by the Carbon Dioxide Research Division, U.S. Department of Energy, under contract DE-AC05-84OR21400 with Martin Marietta Systems, Inc. (subcontracts 19X-SC166C to J. Sarmiento and 19X-SC165V to U. Siegenthaler).

REFERENCES

Alexander, R. C., and R. L. Mobley, Monthly average sea surface temperatures and ice pack limits on a 1° global grid, *Mon. Weather Rev., 104*, 143–148, 1976.

Bacastow, R. B., Numerical evaluation of the evasion factor, in *Carbon Cycle Modeling*, edited by B. Bolin, pp. 95–101, John Wiley, New York, 1981.

Bacastow, R. B., and E. Maier-Reimer, Ocean-circulation model of the carbon cycle, *Clim. Dyn., 4*, 95–125, 1990.

Baes, C. F., Jr., A. Björkström and P. J. Mulholland, Uptake of carbon dioxide by the oceans, in *Atmospheric Carbon Dioxide and the Global Carbon Cycle*, edited by J. R. Trabalka, U.S. Department of Energy, Carbon Dioxide Research Division, Washington, D.C., 1985.

Beardsmore, D. J., and G. I. Pearman, Atmospheric carbon dioxide measurements in the Australian region, data from surface observatories, *Tellus, 39B*, 459–476, 1987.

Bolin, B., A.Björkström, K. Holmen, and B. Moore, On inverse methods for combining chemical and physical oceanographic data, a steady-state analysis of the Atlantic Ocean, *Rep. CM-71*, 189 pp., Dep. of Meteorol., Univ. of Stockholm, Int. Meteorol. Inst., Stockholm, 1987.

Brewer, P. G., Direct observation of the oceanic CO_2 increase, *Geophys. Res. Lett., 5*, 997–1000, 1978.

Brewer, P. G., C. Goyet, and D. Dyrssen, Carbon dioxide transport by ocean currents at 25°N latitude in the Atlantic Ocean, *Science, 246*, 477–479, 1989.

Broecker, W.S., T.H. Peng, *Tracers in the Sea*, Eldigio Press, Palisades, New York, 1982.

Broecker, W.S., T.H. Peng, G. Ostlund, and M. Stuiver, The distribution of bomb radiocarbon in the ocean, *J. Geophys. Res., 90*, 6953–6970, 1985*a*.

Broecker, W. S., T. Takahashi, and T.-H. Peng, Reconstruction of past atmospheric CO_2 contents from the chemistry of the contemporary ocean, an evaluation, *DOE Tech. Rep. DOE/OR-857*, 79 pp., U. S. Dep. of Energy, Washington, D. C., 1985*b*.

Bryan, K., A numerical method for the study of the circulation of the world ocean, *J. Comput. Phys., 4*, 347–376, 1969.

Bryan, K., Accelerating the convergence to equilibrium of ocean climate models, *J. Phys. Oceanogr., 14*, 666–673, 1984.

Bryan, K., S. Manabe, and R. C. Pacanowski, A global ocean-atmosphere climate model, Part II, The oceanic circulation, *J. Phys. Oceanogr., 5*, 30–46, 1975.

Callendar, G. S., The artificial production of carbon dioxide and its influence on temperature, *Q. J. R. Meteorol. Soc., 64*, 223–240, 1938.

Callendar, G. S., Variations in the amount of carbon dioxide in different air currents, *Q. J. R. Meteorol. Soc., 66*, 395–400, 1940.

Callendar, G. S., Can carbon dioxide influence climate?, *Weather, 4*, 310–314, 1949.

Chen, C.-T., On the distribution of anthropogenic CO_2 in the Atlantic and Southern Oceans, *Deep Sea Res., 29*, 563–580, 1982*a*.

Chen, C.-T., Oceanic penetration of excess CO_2 in a cross section between Alaska and Hawaii, *Geophys. Res. Lett., 9*, 117–119, 1982*b*.

Chen, C.-T., Carbonate chemistry of the Weddell Sea, *DOE tech. rep., DOE/EV/10611-4*, 118 pp., U. S. Dep. of Energy, Washington, D. C., 1984.

Chen, C.-T., and E. T. Drake, Carbon dioxide increase in the atmosphere and oceans and possible effects on climate, *Annu. Rev. Earth Planet. Sci., 14*, 201–235, 1986.

Chen, C.-T., and F. J. Millero, Gradual increase of oceanic CO_2, *Nature, 277*, 205–206, 1979.

Chen, C.-T., and A. Poisson, Excess carbon dioxide in the Weddell Sea, *Antarc. J. U.S., 19*, 74–75, 1984.

Chen, C.-T., and R. M. Pytkowicz, On the total CO_2-titration alkalinity-oxygen system in the Pacific Ocean, *Nature, 281*, 362–365, 1979.

Chen, C.-T., F. J. Millero, and R. M. Pytkowicz, Comment on calculating the oceanic CO_2 increase, a need for caution by A. M. Shiller, *J. Geophys. Res., 87*, 2083–2085, 1982.

Chen, C.-T., C. L. Wei, and M. R. Rodman, Carbonate chemistry of the Bering Sea, *DOE tech. rep., DOE/EV/10611-5*, 79 pp., U. S. Dep. of Energy, Washington, D. C., 1985.

Chen, C.-T., M. R. Rodman, C.-L. Wei, and E. J. Olson, Car-

bonate chemistry of the North Pacific Ocean, *DOE tech. rep., DOE/NBB-0079*, 176 pp., U. S. Dep. of Energy, Washington, D. C., 1986.

Conway, T. J., P. Tans, L. S. Waterman, K. W. Thoning, K. A. Masarie, and R. H. Gammon, Atmospheric carbon dioxide measurements in the remote global troposphere, 1981–1984, *Tellus, 40B*, 81–115, 1988.

Enting, I. G., and J. V. Mansbridge, Seasonal sources and sinks of atmospheric CO_2 direct inversion of filtered data, *Tellus, 41B*, 111–126, 1989.

Erickson, D. J., III, Variations in the global air-sea transfer velocity field of CO_2, *Global Biogeochem. Cycles, 3*, 37–41, 1989.

Esbensen, S.K., and Y. Kushnir, The heat budget of the global ocean, An atlas based on estimates from surface marine observations,*Rep. 29*, Climate Research Institute, Oregon State University, Corvallis, Oregon, 1981.

Etcheto, J., and L. Merlivat, Satellite determination of the carbon dioxide exchange coefficient at the ocean-atmosphere interface, a first step, *J. Geophys. Res., 93*, 15,669–15,678, 1988.

Fink, R., Contributions to the carbon cycle, 1, Influence of uncertainties in the carbonate equilibrium constant, 2, A two-dimensional diffusion model of the ocean, Diploma thesis, Physics Institute, University of Bern, 1991.

Friedli, H., H. Lötscher, H. Oeschger, U. Siegenthaler, and B. Stauffer, Ice core record of the $^{13}C/^{12}C$ ratio of atmospheric carbon dioxide in the past two centuries, *Nature, 324*, 237–238, 1986.

Fung, I. Y., C. J. Tucker, and K. C. Prentice, Application of advanced very high resolution radiometer vegetation index to study atmosphere-biosphere exchange of CO_2, *J. Geophys. Res., 92*, 2999–3015, 1987.

Goldman J. C., and M. R. Dennett, Carbon dioxide exchange between air and seawater, no evidence for rate catalysis, *Science, 220*, 199–201, 1983.

Goyet, C., and A. Poisson, New determination of carbonic acid dissociation constants in seawater as a function of temperature and salinity, *Deep Sea Res., 36*, 1635–1654, 1989.

Harvey, L. D. D., Managing Atmospheric CO_2, *Clim. Change, 15*, 343–381, 1989.

Hasselmann, K., An ocean model for climate variability studies, *Progr. Oceanogr., 11*, 69–92, 1982.

Heimann, M., and C. D. Keeling, A three-dimensional model of atmospheric CO_2 transport based on observed winds, 2, Model description and simulated tracer experiments, in *Aspects of Climate Variability in the Pacific and the Western Americas, Geophys. Monogr. 55*, edited by D. H. Peterson, pp. 237–275, AGU, Washington, D. C., 1989.

Heimann, M., and P. Monfray, Spatial and temporal variation of the gas exchange coefficient for CO_2; 1, Data analysis and global validation, *Report No. 31*, 29 pp., Max-Planck-Institut für Meterologie , Hamburg, Germany, 1989.

Heimann, M., C. D. Keeling, and I. Y. Fung, Simulating the atmospheric carbon dioxide distribution with a three-dimensional tracer model, in *The Changing Carbon Cycle: A Global Analysis*, edited by J. R. Trabalka and D. E. Reichle, pp. 16–49, Springer-Verlag, New York, 1986.

Hellerman, S., and M. Rosenstein, Normal monthly wind stress over the world ocean with error estimates, *J. Phys. Oceanogr., 13*, 1093–1104, 1983.

Houghton, J. T., G. J. Jenkins, and J. J. Ephraums, *Climate Change, The IPCC Scientific Assessment*, 365 pp., Cambridge University Press, New York, 1990.

Jacob, D. J., M. J. Prather, S. C. Wofsy, and M. B. McElroy, Atmospheric distribution of ^{85}Kr simulated with a general circulation model, *J. Geophys. Res., 92*, 6614–6626, 1987.

Joos, F., J. L. Sarmiento, and U. Siegenthaler, Estimates of the effect of Southern Ocean iron fertilization on atmospheric CO_2 concentrations, *Nature, 349*, 772–774, 1991.

Keeling, C.D., Carbon dioxide in surface ocean waters, 4, Global distribution, *J. Geophys. Res., 73*, 4543–4553, 1968.

Keeling, C. D., and M. Heimann, Meridional eddy diffusion model of the transport of atmospheric carbon dioxide, 2, Mean annual carbon cycle, *J. Geophys. Res., 91*, 7782–7798, 1986.

Keeling, C. D., R. B. Bacastow, A. F. Carter, S. C. Piper, T. P. Whorf, M. Heimann, W. G. Mook, and H. Roeloffzen, A three dimensional model of atmospheric CO_2 transport based on observed winds, 1, Analysis of observational data, in *Aspects of Climate Variability in the Pacific and the Western Americas*, edited by D. H. Peterson, pp. 165–236, Geophys. Monogr. 55, AGU, Washington , D. C., 1989*a*.

Keeling, C. D., S. C. Piper, and M. Heimann, A three dimensional model of atmospheric CO_2 transport based on observed winds, 4, Mean annual gradients and interannual variations, in *Aspects of Climate Variability in the Pacific and the Western Americas*, Geophys. Monogr. 55, edited by D. H. Peterson, pp. 305–363, AGU, Washington , D. C., 1989*b*.

Knox, F., and M. McElroy, Changes in atmospheric CO_2, influence of the marine biota at high latitudes, *J. Geophys. Res., 89*, 4629–4637, 1984.

Levitus, S., Climatological Atlas of the World Ocean, *NOAA Prof. Pap. 13*, 173 pp., U.S. Govt. Printing Office, Washington, D.C., 1982.

Liss, P., and L. Merlivat, Air-sea gas exchange rates, introduction and synthesis. in *The Role of Air-Sea Exchange in Geochemical Cycling*, edited by P. Buat-Ménard, pp. 113–128, D. Reidel, Hingham, Mass., 1986.

Lyman, J., Buffer mechanisms of seawater, Ph.D. thesis, University of California, Los Angeles, Calif., 1956.

Maier-Reimer, E., and K. Hasselmann, Transport and storage of CO_2 in the ocean – An inorganic ocean-circulation cycle model, *Clim. Dyn., 2*, 63–90, 1987.

Maier-Reimer, E., K. Hasselmann, D. Olbers, and J. Willebrand, An ocean circulation model for climate studies, *Tech. Rep.*, Max-Planck-Institut für Meteorologie, Hamburg, Germany, 1982.

Marland, G., Fossil fuels CO_2 emissions, *CDIAC Communications, Winter 1989*, pp. 1–3, Carbon Dioxide Information Analysis Center, Oak Ridge National Laboratory, Oak Ridge, Tenn., 1989.

Mehrbach, C., C. H. Culberson, J. E. Hawley, and R. M. Pytkowicz, Measurement of apparent dissociation constants of carbonic acid in seawater at atmospheric pressure, *Limnol. Oceanogr., 18*, 897–907, 1973.

Memery, L., and L. Merlivat, Influence of gas transfer on the CO_2 uptake by the ocean, *J. Geophys. Res., 90*, 7361–7366, 1985.

Monfray, P., Echanges océan/atmosphère du gaz carbonique, variabilité avec l'état de la mer, Thesis, Docteur des sciences physiques, Univ. de Picardie, Saint-Quentin, France, 1987.

Monfray, P., M. Heimann, and E. Maier-Reimer, Uptake of anthropogenic CO_2 by ocean models calibrated or tested by bomb radiocarbon, sensitivity to uncertainties in gas exchange formulation and ^{14}C data, in *Extended Abstracts of Papers Presented at the Third International Conference on Analysis and Evaluation of Atmospheric CO_2 Data Present and Past, Environmental Pollution Monitoring and Research Programme, Rep. 59*, World Meteorological Organization, Geneva, 1989.

Najjar, R. G., Simulations of the phosphorus and oxygen cycles in the world ocean using a general circulation model, Ph. D. thesis, Princeton University, Princeton, N. J., 1990.

Neftel, A., E. Moor, H. Oeschger, and B. Stauffer, Evidence from polar ice cores for the increase in atmospheric CO_2 in the past two centuries, *Nature, 315*, 45–47, 1985.

Oeschger, H., U. Siegenthaler, U. Schotterer, and A. Gugelmann, A box diffusion model to study the carbon dioxide exchange in nature, *Tellus, 27*, 168–192, 1975.

Peng, T.-H., and W. S. Broecker, Dynamical limitations on the Antarctic iron fertilization strategy, *Nature, 349*, 227–229, 1991.

Peng, T.-H., T. Takahashi, and W. S. Broecker, Seasonal variability of carbon dioxide, nutrients and oxygen in the northern North Atlantic surface water, observations and a model, *Tellus, 39B*, 439–458, 1987.

Prather, M., M. McElroy, S. Wofsy, G. Russell, and D. Rind, Chemistry of
the global troposphere, fluorocarbons as tracers of air motion, *J. Geophys. Res., 92*, 6579–6613, 1987.

Raynaud, D., and J. M. Barnola, An Antarctic ice core reveals atmospheric CO_2 variations over the past few centuries, *Nature, 315*, 309–311, 1985.

Rotty, R.M., and C.D. Masters, Carbon dioxide from fossil fuel combustion, trends, resources, and technological implications, in *Atmospheric Carbon Dioxide and the Global Carbon Cycle*,

edited by J. Trabalka, pp. 63–80, DOE/ER-0239, U.S. Department of Energy, Carbon Dioxide Research Division, Washington, D.C., 1985.

Sarmiento, J. L., A simulation of bomb tritium entry into the Atlantic Ocean, *J. Phys. Oceanogr., 13*, 1924–1939, 1983.

Sarmiento, J. L., and J. R. Toggweiler, A new model for the role of the oceans in determining atmospheric pCO_2 *Nature, 308*, 621–624, 1984.

Sarmiento, J. L., M. J. R. Fasham, R. Slater, J. R. Toggweiler, and H. Ducklow The role of biology in the chemistry of CO_2 in the ocean, in *Chemistry of the Greenhouse Effect*, edited by M. Farrell, Lewis Publ., N.Y., *in press*, 1989.

Shiller, A. M., Calculating the oceanic CO_2 increase, a need for caution, *J. Geophys. Res., 86*, 11,083–11,088, 1981.

Shiller, A. M., Reply, *J. Geophys. Res., 87*, 2086, 1982.

Siegenthaler, U., Uptake of excess CO_2 by an outcrop-diffusion model of the ocean, *J. Geophys. Res., 88*, 3599–3608, 1983.

Siegenthaler, U., Carbon dioxide, its natural cycle and anthropogenic perturbation, in *The Role of Air-Sea Exchange in Geochemical Cycling*, edited by P. Buat-Ménard, pp. 209–248, D. Reidel , Hingham, Mass, 1986.

Siegenthaler, U., and H. Oeschger, Biospheric CO_2 emissions during the past 200 years reconstructed by deconvolution of ice core data, *Tellus, 39B*, 140–154, 1987.

Siegenthaler, U., and T. Wenk, Rapid atmospheric CO_2 variations and ocean circulation, *Nature, 308*, 624–625, 1984.

Siegenthaler, U., H. Friedli, H. Loetscher, E. Moor, A. Neftel, H. Oeschger, and B. Stauffer, Stable-isotope ratios and concentration of CO_2 in air from polar ice cores, *Ann. Glaciol., 10*, 1–6, 1988.

Spitzer, W. S., and W. J. Jenkins, Rates of vertical mixing, gas exchange and new production, estimates from seasonal gas cycles in the upper ocean near Bermuda, *J. Mar. Res., 47*, 169–196, 1989.

Takahashi, T., P. Kaiteris, W. S. Broecker, and A. E. Bainbridge, An evaluation of the apparent dissociation constants of carbonic acid in seawater, *Earth Planet. Sci. Lett., 32*, 458–467, 1976.

Takahashi, T., D. Chipman, and T. Volk, Geographical, seasonal, and secular variations of the partial pressure of CO_2 in surface waters of the North Atlantic Ocean, the results of the North Atlantic TTO Program, in *Proceedings, Carbon Dioxide Research Conference, Carbon Dioxide, Science and Consensus, CONF-820970*, U. S. Dep. of Energy, Washington, D. C., 1983.

Tans, P. P., T. J. Conway, and T. Nakazawa, Latitudinal distribution of the sources and sinks of atmospheric carbon dioxide derived from surface observations and an atmospheric transport model, *J. Geophys. Res., 94*, 5151–5172, 1989.

Tans, P. P., I. Y. Fung, and T. Takahashi, Observational constraints on the global atmospheric CO_2 budget, *Science, 247*, 1431–1438, 1990.

Thomas, F., C. Perigaud, L. Merlivat, and J. F. Minster, World scale monthly mapping of the CO_2 ocean-atmosphere gas transfer coefficient, *Philos. Trans. R. Soc. London, Ser., A, 325*, 71–83, 1988.

Toggweiler, J.R., K. Dixon, and K. Bryan, Simulations of radiocarbon in a coarse-resolution, world ocean model, I, Steady state, pre-bomb distributions, *J. Geophys. Res., 94*, 8217–8242, 1989*a*.

Toggweiler, J.R., K. Dixon, and K. Bryan, Simulations of radiocarbon in a coarse-resolution, world ocean model, II, Distributions of bomb-produced ^{14}C, *J. Geophys. Res., 94*, 8243–8264, 1989*b*.

Volk, T., and R. Bacastow, The changing patterns of δpCO_2 between the ocean and atmosphere, *Global Biogeochem. Cycles, 3*, 179–189, 1989.

Wanninkhof, R., Relationship between wind speed and gas exchange over the ocean, *J. Geophys. Res.*, in press, 1992.

Watson, A. J., R. C. Upstill-Goddard, and P. S. Liss, Air-sea gas exchange in rough and stormy seas measured by a dual-tracer technique, *Nature, 349*, 145–147, 1991*a*.

Watson, A. J., C. Robinson, J. E. Robinson, P. J. le B. Williams, and M. J. R. Fasham, Spatial variability in the sink for atmospheric carbon dioxide in the North Atlantic, *Nature, 350*, 50–53, 1991*b*.

Weiss, R.F., Carbon dioxide in water and sea water, The solubility of a non-ideal gas, *Mar. Chem., 2*, 203–215, 1974.

Wong, C. S., and Y.-H. Chan, Temporal variations in the partial pressure and flux of CO_2 at ocean station P in the subarctic northeast Pacific Ocean, *Tellus, 43B*, 206–223, 1991.

J.C. Orr and J.L. Sarmiento, Program in Atmospheric and Oceanic Sciences, Princeton University, Princeton, NJ 08544.

U. Siegenthaler, Physics Institute, University of Bern, Bern, Switzerland.

(Received October 12, 1990;
revised October 1, 1991;
accepted October 15, 1991.)